

NPS ARCHIVE  
1966  
SHEEHAN, J.

MEASUREMENT OF ACOUSTICAL IMPEDANCES  
OF FLUIDS BY ANALYSIS OF TRANSIENT  
ACOUSTIC WAVE-SHAPES USING AN  
ACOUSTICAL WAVEGUIDE WITH  
PIEZOELECTRIC TRANSDUCERS

JAMES EDWARD SHEEHAN

DUDLEY KNOX LIBRARY  
NAVAL POSTGRADUATE SCHOOL  
MONTEREY, CA 93943-5101

L  
NAVAL POSTGRADUATE SCHOOL  
MONTEREY, CALIF. 93943









MEASUREMENT OF ACOUSTICAL IMPEDANCES OF FLUIDS BY  
ANALYSIS OF TRANSIENT ACOUSTIC WAVESHAPES USING AN  
ACOUSTICAL WAVEGUIDE WITH PIEZOELECTRIC TRANSDUCERS.

by

James Edward Sheehan

//

NO FORN

Submitted in partial fulfillment

for the degree of

MASTER OF SCIENCE IN PHYSICS

from the

UNITED STATES NAVAL POSTGRADUATE SCHOOL

May 1966

# ABSTRACT

A method has been developed for measuring the acoustic impedance of fluids in a fluid-filled waveguide terminated at each end by piezoelectric crystals. Output voltage waveforms were computed for the general case of an arbitrary driving voltage. Analysis of these output waveforms, when the driving voltage was an impulse function, indicated significant changes in the voltage envelopes as the acoustic impedance of the fluid within the waveguide was varied. The time of the first and second phase changes in the second received echo were plotted as a function of fluid impedance. Test fluids were analyzed with an impedance range of from  $0.66 \times 10^6$  rayls to  $19.7 \times 10^6$  rayls. The experimental results using the time of the second axis crossing or phase change as the test criterion, indicated that the acoustic impedance can be measured with the following accuracies:

- a. 0.5 percent in the neighborhood of  $Z = 0.66 \times 10^6$  rayls.
- b. 0.9 percent in the neighborhood of  $Z = 1.50 \times 10^6$  rayls.
- c. 2.0 percent in the neighborhood of  $Z = 2.50 \times 10^6$  rayls.



TABLE OF CONTENTS

Section	Page
1. Introduction	9
2. Theory	9
3. Theoretically Predicted Waveforms	20
4. Design of Apparatus and Associated Equipment	22
5. Discussion of Results	26
6. Error Analysis	47
7. Data Evaluation and Conclusions	49
8. Acknowledgements	54
APPENDIX I	57
APPENDIX II	61
APPENDIX III	62

COBBLESTONE LIBRARY  
A SMALL PICTURE IN THE BOOK  
MONTICELLO, VA 22952

## LIST OF TABLES

Table		Page
I	Associated Electrical Equipment	26
II	Various Fluids and their Acoustical Impedances	26



# LIST OF ILLUSTRATIONS

Figure	Page
1. Growth of Pressure patterns	15
2. Relative Output Voltage vs. Resistance	21
3. Cutaway Drawing of Acoustical Waveguide	23
4. Associated Electrical Equipment	25
5. $E_1^0$ (COMPUTED) for Distilled Water at T=21 degrees C.	28
6. $E_1^2$ (COMPUTED) for Distilled Water at T=21 degrees C.	29
7. $E_1^4$ (COMPUTED) for Distilled Water at T=21 degrees C.	30
8. $E_1^6$ (COMPUTED) for Distilled Water at T=21 degrees C.	31
9. $E_1^8$ (COMPUTED) for Distilled Water at T=21 degrees C.	32
10. Photograph of the waveform $E_1^0$ for distilled water at T=21 degrees C.	33
11. Photograph of the waveform $E_1^2$ for distilled water at T=21 degrees C.	34
12. Photograph of the waveform $E_1^4$ for distilled water at T=21 degrees C.	35
13. Photograph of the waveform $E_1^6$ for distilled water at T=21 degrees C.	36
14. Photograph of the waveform $E_1^8$ for distilled water at T=21 degrees C.	37
15. $E_1^0$ for Distilled Water at T=21 degrees C.	38
16. $E_1^2$ for Distilled Water at T=21 degrees C.	39
17. $E_1^0$ and $E_1^2$ for pentane	41
18. $E_1^0$ and $E_1^2$ for tert-butyl chloride	42
19. $E_1^0$ and $E_1^2$ for acetone	43
20. $E_1^0$ and $E_1^2$ for turpentine	44
21. $E_1^0$ and $E_1^2$ for benzine	45
22. $E_1^0$ for glycerol	46

# LIST OF ILLUSTRATIONS

Figure		Page
23.	$E_1^0$ for mercury	46
24.	Acoustical Impedance vs. Time for	51
	a. FIRST AXIS CROSSING	
	b. SECOND AXIS CROSSING	
25.	Acoustical Impedance vs. Time to First axis crossing	52
26.	Acoustical Impedance vs. Time to Second axis crossing	53

## 1. Introduction.

A fluid-filled waveguide, terminated at each end by a piezoelectric transducer, and excited with acoustic transients, was examined as a means of measuring the specific acoustic resistance of the test fluid. When the transmitting crystal is activated by a narrow rectangular pulse, the resultant output voltage pulse shapes are strongly dependent upon the specific acoustic resistance,  $\rho c$ , of the fluid that fills the guide. By recording the pertinent characteristics of the output waveforms for many fluids of widely varying acoustic impedance, it is possible to determine the value of  $\rho c$  for an unknown fluid.

If the waveguide were used in conjunction with pressure and temperature measuring devices, measurements of the salinity of sea water at depth in the oceans would be possible. Since the present method for determining salinity of sea water is first to withdraw a sample and then to test it chemically, the advantages of this suggested method are obvious.

Expressions for the output voltage waveforms at the receiving crystal, when the transmitting crystal is driven by an arbitrary voltage, are developed in Sections 2 and 3. These expressions are valid for any fluid and are compared with experimental results for fluids whose acoustic impedances range from  $0.66 \times 10^6$  rayls to  $19.7 \times 10^6$  rayls in Section 5. The results are analyzed and a means for measuring acoustic impedance with an accuracy of better than 1.0 percent is shown in Section 7.

## 2. Theory.

The theory that was developed here is similar to some previous

work done by Redwood[1], Cook[2], Huntington[3], and Coppens[4], among others. Redwood's treatment of the acoustical delay line as a transmission line led to equivalent circuits which are only approximate electrical analogs for the plate transducer. Cook used Laplace transforms and obtained the equivalent mechanical analog for piezoelectric transducers. Huntington also devised an equivalent electrical circuit for piezoelectric transducers. The theoretical development presented here parallels the approach used by Coppens. Whereas Coppens was concerned primarily with the velocity propagation from a vacuum-backed crystal, this theory is concerned with pressures generated and received by crystals with media of arbitrary impedances on both sides of the crystals.

The general equations relating stress and voltage for a piezoelectric crystal will be used to develop expressions for the pressure output of a transmitting crystal, and the voltage output of another crystal receiving the resulting pressure wave. In addition, expressions for the successively reflected pressure packets will be obtained which will enable one to derive expressions for successive output voltage functions. These expressions were obtained for an x-cut quartz crystal, operating in a thickness mode of vibration, with an arbitrary voltage  $V(t)$  applied. It will be assumed that losses in the crystal and loading medium may be neglected, and that the thickness mode is the only mode appreciably excited, so that only displacements in the X-direction are of significance.

The basic equations for piezoelectric action with the above assumptions are [3]



$$V(t) = h \{ \xi(d,t) - \xi(0,t) \} + \sigma(t) \frac{4\pi d}{\epsilon} \quad (1)$$

$$S(x) = \rho c^2 \frac{\partial \xi}{\partial x} + h \sigma(t) \quad (2)$$

where the defining terms in the above equation are as follows.

$V(t)$  = applied voltage

$h$  = appropriate piezoelectric stress constant

$\xi$  = particle displacement

$\sigma(t)$  = free surface charge density

$d$  = thickness of the crystal

$\epsilon$  = dielectric constant of the crystal

$S(x)$  = stress

$\rho$  = density of the crystal

$c$  = velocity of sound in the crystal

It has been shown [4] that for quartz acting as a transmitter,

$$h \{ \xi(d,t) - \xi(0,t) \} \ll \frac{\sigma(t) 4\pi d}{\epsilon} .$$

Equation 1 then becomes

$$V(t) = \sigma(t) \frac{4\pi d}{\epsilon} . \quad (3)$$

Solving Eq. 3 for  $\sigma(t)$  and letting

$$a = \frac{\epsilon d}{4\pi d} \quad (4)$$

Eq. 2 can be expressed as

$$S(x) = \rho c^2 \frac{\partial \xi}{\partial x} + a V(t) . \quad (5)$$

If  $\xi^+$  represents a wave traveling the +x direction and  $\xi^-$  a wave traveling in the -x direction, then

$$c \frac{\partial \xi}{\partial x} = \mp \frac{\partial \xi}{\partial t} \quad (6)$$

from the wave equation,  $\frac{\partial^2 \xi}{\partial t^2} = c^2 \frac{\partial^2 \xi}{\partial x^2}$ .

Use of the following notation:

MEDIUM 1	CRYSTAL	MEDIUM 2
$Z_1 = \rho_1 c_1$	$Z = \rho c$	$Z_2 = \rho_2 c_2$
$M_1 = \frac{Z_1}{Z}$		$M_2 = \frac{Z_2}{Z} \quad (7)$
$\xi_1 = \xi_1^+ + \xi_1^-$	$\xi = \xi^+ + \xi^-$	$\xi_2 = \xi_2^+ + \xi_2^-$

and the boundary conditions of continuity of displacement,

$$\xi_1(0, t) = \xi(0, t), \quad (8-a)$$

$$\xi(d, t) = \xi_2(d, t), \quad (8-b)$$

and continuity of stress,

$$S_1(0) = S(0), \quad (8-c)$$

$$S_2(d) = S(d), \quad (8-d)$$

together with Eqs. 5 and 6 results in

$$Z_1 \frac{\partial}{\partial t} \{ \xi_1^+(0, t) - \xi_1^-(0, t) \} = Z \frac{\partial}{\partial t} \{ \xi^+(0, t) - \xi^-(0, t) \} - a V(t) \quad (9-a)$$

and

$$Z_2 \frac{\partial}{\partial t} \{ \xi_2^+(d, t) - \xi_2^-(d, t) \} = Z \frac{\partial}{\partial t} \{ \xi^+(d, t) - \xi^-(d, t) \} - a V(t) \quad (9-b)$$

By addition and subtraction of Eqs. 9-a and 9-b, and the use of the relationship  $\bar{p} = Z \frac{\partial \xi}{\partial t}$ , the following pressure relationships are obtained:

$$\bar{p}^-(0,t) = \frac{M_1}{1+M_1} a V(t), \quad (10-a)$$

$$\bar{p}^+(0,t) = -\frac{1}{1+M_1} a V(t), \quad (10-b)$$

$$\bar{p}^-(d,t) = -\frac{1}{1+M_2} a V(t), \quad (10-c)$$

and 
$$\bar{p}^+(d,t) = \frac{M_2}{1+M_2} a V(t). \quad (10-d)$$

If one uses the following definitions,

$$V(t) = V(t - 2d/c),$$

$$\bar{p}(t) = \bar{p}(t - 2d/c),$$

$$R_{(j)} = \frac{Z_j - Z}{Z_j + Z} = \frac{M_j - 1}{M_j + 1}, \quad (\text{pressure reflection coefficient})$$

$$T_{(j)} = \frac{2Z_j}{Z_j + Z} = \frac{2M_j}{M_j + 1}, \quad (\text{pressure transmission coefficient})$$

where  $j$  indicates either surface 1 ( $X=0$ ) or 2 ( $X=d$ ) and  $i$  is an integer, then Eqs. 10-a through 10-d become

$$\bar{p}^-(0,t) = \bar{p}^-(0,t), \quad (11-a)$$

$$\bar{p}^+(0,t) = -\frac{1}{M_1} \bar{p}^-(0,t), \quad (11-b)$$

$$\bar{p}^-(d,t) = -\frac{1}{M_2} \frac{T_2}{T_1} \bar{p}^-(0,t), \quad (11-c)$$

and 
$$\bar{p}^+(d,t) = \frac{T_2}{T_1} \bar{p}^-(0,t). \quad (11-d)$$

According to this analysis, when a voltage function is impressed across the crystal transmitter, each face of the crystal acts like a pressure generating device and sends a pressure wave into both the crystal and the adjacent medium. The magnitude of each of the four pressure waves is determined by the acoustic impedances of the two media at the relevant boundary. It should be noted that the pulses sent into the crystal are of like phase; they are, however, of opposite phase to those sent into the surrounding media. This is indicated in the following diagram.

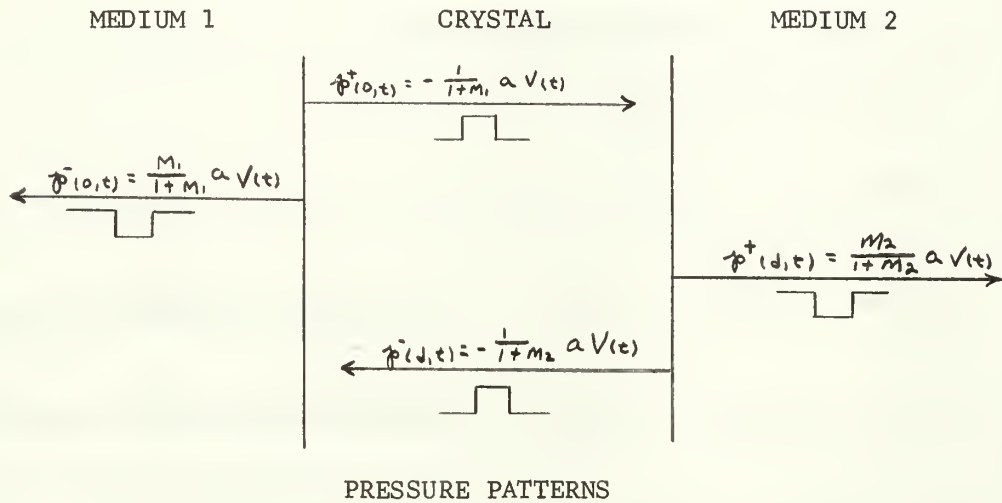


Figure 1 is a graphical development of the growth of a pressure waveform resulting from a single voltage impulse impressed on the crystal. At time zero, four pulses are generated. From surface 1,  $\bar{p}(0,t)$  is sent into medium 1 and  $-\frac{1}{M_1} \bar{p}(0,t)$  is sent into the crystal. From surface 2,  $\frac{M_2}{1+M_2} \bar{p}(0,t)$  is sent into medium 2 and  $-\frac{1}{M_1} \frac{M_2}{1+M_2} \bar{p}(0,t)$  is sent into the crystal. As time increases, each of the two pulses sent into the crystal is repeatedly reflected between the faces of the crystal. At each reflection, some energy is transmitted into the adjacent medium.



Figure 1. Growth of Pressure Patterns.

After a time  $d/c$ , the wave which started at surface 2 is partially reflected at surface 1 and the portion transmitted into medium 1 is  $T_1 \left\{ -\frac{1}{M_2} \frac{T_2}{T_1} \hat{p}(0, t) \right\}$ . After a time  $2d/c$ , the wave which started at surface 1 has been reflected by surface 2 and is now at surface 1. The portion now transmitted into medium 1 is  $T_1 R_2 \left\{ -\frac{1}{M_2} \hat{p}(0, t) \right\}$ ; that transmitted into medium 1 at time  $3d/c$  is  $T_1 R_1 R_2 \left\{ -\frac{1}{M_2} \frac{T_2}{T_1} \hat{p}(0, t) \right\}$ . The resultant waveform sent into medium 1 is therefore, a series of impulses of varying amplitude and phase, each separated in time by  $d/c$ , the time of flight of sound in the crystal. This series can be expressed as

$$\begin{aligned} \hat{p}_1^0(0, t) = & \frac{M_1}{1+M_1} a V(0) + T_1 \left\{ -\sum_{i=0}^{\infty} \frac{1}{1+M_2} a V(\lambda + \frac{1}{2}) (R_1 R_2)^i \right. \\ & \left. - \sum_{i=1}^{\infty} \frac{1}{1+M_1} a V(\lambda) \frac{(R_1 R_2)^i}{R_1} \right\}. \end{aligned} \quad (12)$$

In the above equation, the subscript for the pressure indicates the crystal at which the pressure acts. The receiving crystal is numbered 1 and the generating crystal numbered 2. The superscript indicates the number of times the entire packet has been reflected. As a further example,  $\hat{p}_1^2$  is the pressure at the receiving crystal (numbered 1) which has been reflected twice, once from the receiving crystal and again from the transmitting crystal so that it is detected at the receiver after three trips through the test fluid. The same notation will be used for the generated voltages:  $E_1^0$  is the voltage generated at the receiving crystal from the initial pressure packet  $\hat{p}_1^0$ ,  $E_1^2$  is the voltage generated at the receiver due to  $\hat{p}_1^2$ , the third generated voltage is  $E_1^4$ , etc.

Equation 12 is in agreement with Eq. 11 of Cook [2] as used in his Fig. 4, and with Eq. 7.11 of Coppens [4] when the appropriate simplifications are made for vacuum backing.

Employment of the same technique as represented in Fig. 1 to derive the expression for  $p'_1$ , yields

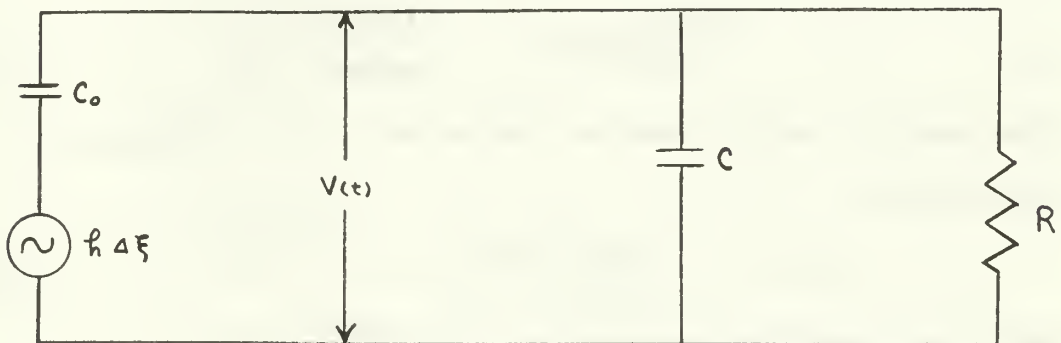
$$p'_1 = -R_1 p_{1(0)} + \sum_{i=0}^{\infty} \frac{1}{M_1} T_1^2 \frac{(R_1 R_2)^i}{R_1} p_{1(i)}^0, \quad (13)$$

and therefore

$$\begin{aligned} \partial_t \{ \xi_{(d,t)} - \xi_{(o,t)} \} = & - \frac{1}{2 M_1} T_1 \left\{ p_{1(0)}^0 - \sum_{i=0}^{\infty} \frac{T_1}{M_1} (R_1 R_2)^i p_{1(i+\frac{1}{2})}^0 \right. \\ & \left. - \sum_{i=1}^{\infty} \frac{T_1}{M_1} \frac{(R_1 R_2)^i}{R_1} p_{1(i)}^0 \right\} \end{aligned} \quad (14)$$

Equation 14 was derived using the expression  $p = Z \frac{\partial \xi}{\partial t}$  and will be necessary in solving for the output voltage  $E_1^0$ .

If we consider the external load of the receiving crystal to be a coaxial cable and voltage amplifier, the equivalent circuit and the defining terms of the crystal and load are as shown below:



where  $Co = \frac{A\epsilon}{4\pi d}$  the capacitance of the crystal

$A$  = the electrode area of the crystal

$C$  = external shunt capacitance

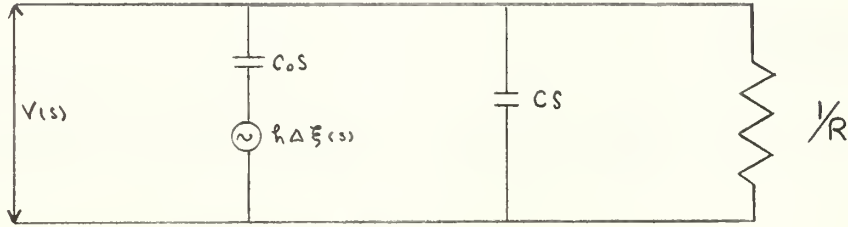
$R$  = external circuit resistance

$$\Delta \xi = \xi_{(d,t)} - \xi_{(o,t)}$$

$$\dot{\Delta \xi} = \frac{\partial}{\partial t} \{ \xi_{(d,t)} - \xi_{(o,t)} \}.$$



To derive the voltage response of the equivalent circuit using Laplace transforms, consider the transformed admittance network with all initial conditions zero.[5]



Solving for the currents into the upper node yields the equation

$$(V(s) - h \Delta \xi(s)) s C_0 + V(s) C s + \frac{V(s)}{R} = 0. \quad (15)$$

By denoting the displacement transfer function as

$$H(s) = \frac{V(s)}{\Delta \xi(s)} \quad (16)$$

Eq. 15 can be solved with the result

$$H(s) = \frac{h R C_0 s}{1 + R(C_0 + C) s} = \frac{h R C_0 s / R(C_0 + C)}{\frac{1}{R(C_0 + C)} + s} \quad (17)$$

The velocity transfer function, defined as  $H'(s) = \frac{V(s)}{\Delta \dot{\xi}(s)}$ , is therefore

$$H'(s) = \frac{h R C_0 / R(C_0 + C)}{\frac{1}{R(C_0 + C)} + s} \quad (18)$$

which for simplicity is written as

$$H'(s) = \frac{A}{s + \frac{1}{B}} \quad (19)$$

with  $A = \frac{h R C_0}{B}$  and  $B = R(C_0 + C)$ .

The output of the transformed network is

$$G(s) = F(s) H'(s) \quad (20)$$

Where  $F(s)$  is the transform of the input to the equivalent circuit

$$\Delta \dot{\xi}(t) = \delta(t) \quad (21)$$



When  $f(t)$  is a rectangular pulse of height  $a$ , and duration  $\lambda$ ,  $f(t)$  can be expressed as

$$f(t) = a \cdot 1(t) - a \cdot 1(t-\lambda) \quad (22)$$

$F(s)$  is the Laplace transform of Eq. 20 so that

$$F(s) = \frac{1}{s} - \frac{1}{s} e^{-\lambda s} \quad (23)$$

Substituting Eqs. 19 and 23 into Eq. 20 yields

$$G(s) = \frac{aA}{s(s + \frac{1}{B})} (1 - e^{-\lambda s}) \quad (24)$$

or

$$G(s) = \frac{a h R C_0 / R(C_0 + C)}{s(s + \frac{1}{R(C_0 + C)})} (1 - e^{-\lambda s}) \quad (25)$$

When  $G(s)$  is transformed back into the time domain

the output voltage is obtained:

$$v(t) = g(t) = a h R C_0 (1 - e^{-t/R(C_0 + C)}) (1(t) - 1(t-\lambda)) \quad (26)$$

or

$$v(t) = h R C_0 \dot{\Delta \xi} (1 - e^{-t/R(C_0 + C)}) \quad (27)$$

If we assume that

$$\frac{t}{R(C_0 + C)} \gg 1 \quad (28)$$

then

$$v(t) = h R C_0 \dot{\Delta \xi} \quad (29)$$

Equation 29 says that for the case in question,  $\dot{\Delta \xi}$  being a rectangular pulse and  $R(C_0 + C) \ll 1$ , the output voltage across the external load is directly proportional to the pressure waveform  $P(t)$ . For the experimental work to follow,  $R(C_0 + C) = 1.6 \times 10^{-8}$  and the assumption of Eq. 28 is justified.

As a test of the validity of Eq. 29, a small amplitude test signal was applied to the circuit and the external resistance  $R$  was

varied over a considerable range while noting the relative output voltage  $v(t)$ . The range of  $R$  used was 3 ohms to 1 megohm. The results shown in Fig. 3, show conclusively that the output voltage is indeed proportional to  $R$  in the neighborhood of  $R = 200$  ohms, the experimental value of resistance used. The curve appears to saturate in the neighborhood of  $R = 600$  ohms and has a relatively flat response as  $R$  is increased further. The relative output voltage rising only from 0.48 at  $R = 560$  ohms to 0.54 at  $R = 1$  megohm.

### 3. Theoretically Predicted Waveforms

When Eq. 16 is substituted into Eq. 29, we have

$$E_1^0 = - \frac{kRC_0}{2} \frac{T_1}{M_1} \left\{ \phi_1^0(t) - \sum_{i=0}^{\infty} \frac{T_2}{M_2} (R_1 R_2)^i \phi_1^0(t + i\tau) \right. \\ \left. - \sum_{i=1}^{\infty} \frac{T_1}{M_1} \frac{(R_1 R_2)^i}{R} \phi_1^0(t) \right\}, \quad (30)$$

which is an expression for the voltage developed at the receiving crystal as a result of a pressure packet  $\phi_1^0(t)$  which is traveling from the transmitter to the receiver (subscript 1) and has not been reflected (superscript 0).

Substitution of Eq. 12 into Eq. 30 yields an expression for the generated output voltage waveform in terms of the applied driving voltage. A digital computer was utilized to compute first the individual pressure waveforms, as in Eq. 12, and then using this to compute the final output voltage waveforms using Eq. 30.

When comparing these results with those of Coppens, it was noted that an error exists in his Eq. 7.23, an expression for the first voltage generated at the receiving crystal. This error originates in his Eq. 7.16, the expression for velocities of the crystal boundaries. His equations have  $t_2$ , the amplitude transmission coefficient,

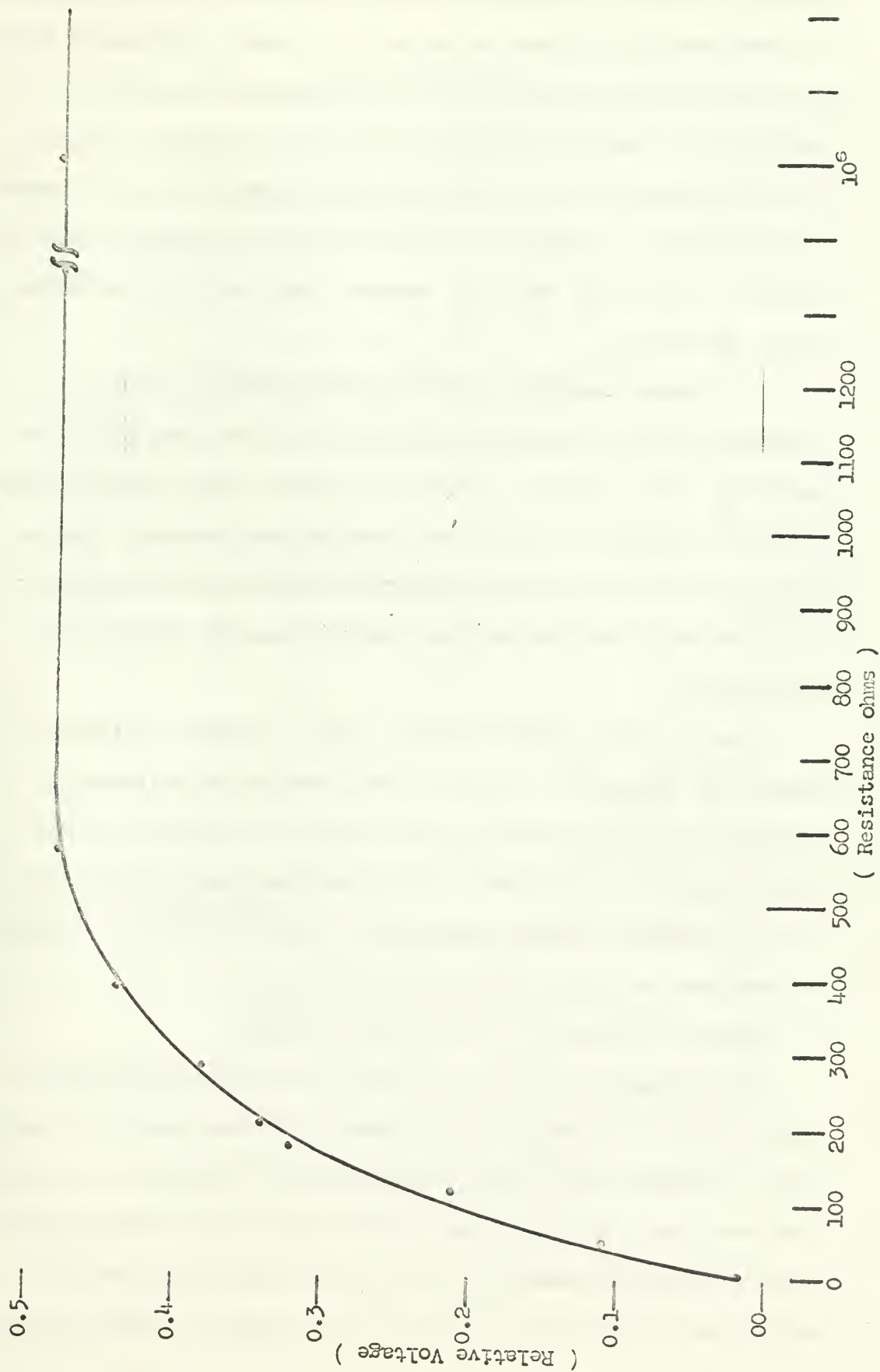


Figure 2. Relative Voltage vs. Resistance.

appearing in both the summation terms. In Eq. 7.23, when he assumes a vacuum backing,  $t_2$  takes the value 2.0. However, the second summation term in Eq. 7.16 should have  $t_1$ , the amplitude transmission coefficient at the fluid boundary, vice  $t_2$  and therefore, his Eq. 7.23 should have  $t_1$  vice 2.0 in the second summation term. Although this effect will be negligible for fluids with an acoustic impedance equal to or less than water, it becomes significant for fluids with higher impedances.

In a manner completely similar to that described by Fig. 1, expressions for the successive reflected pressure waves within the cavity,  $p_1^1$ ,  $p_1^2$ ,  $p_1^3$ , etc., can be obtained. Each of these pressure waves will generate a voltage as it strikes this crystal. The expressions for the succeeding generated voltages can be obtained by utilizing Eq. 30 with appropriate substitutions for the pressure expression  $p_1^0$ .

Using a C.D.C. digital computer 1604, the first 13 pressure packets,  $p_1^0$  through  $p_1^{13}$ , and the first seven output voltages  $E_1^0$  through  $E_1^{12}$  were computed for various fluids. In addition, these output voltage waveforms were plotted and their amplitudes tabulated. The computer program presented in Appendix I is quite flexible and self-explanatory.

#### 4. Design of Apparatus and Associated Equipment

The propagation of sound occurs in the acoustical delay line, shown in Fig. 3, between two 5 mc quartz crystals, spaced 2.0 inches apart in a test cavity of 1.0 inch diameter. The ends of the stainless steel walls that are flush with the plate transducers were constructed with great care to ensure that the faces were parallel to within one one-thousandth of an inch. The acoustic distance for one

Pressure Release and Filling Cavity  
Positioning Screw

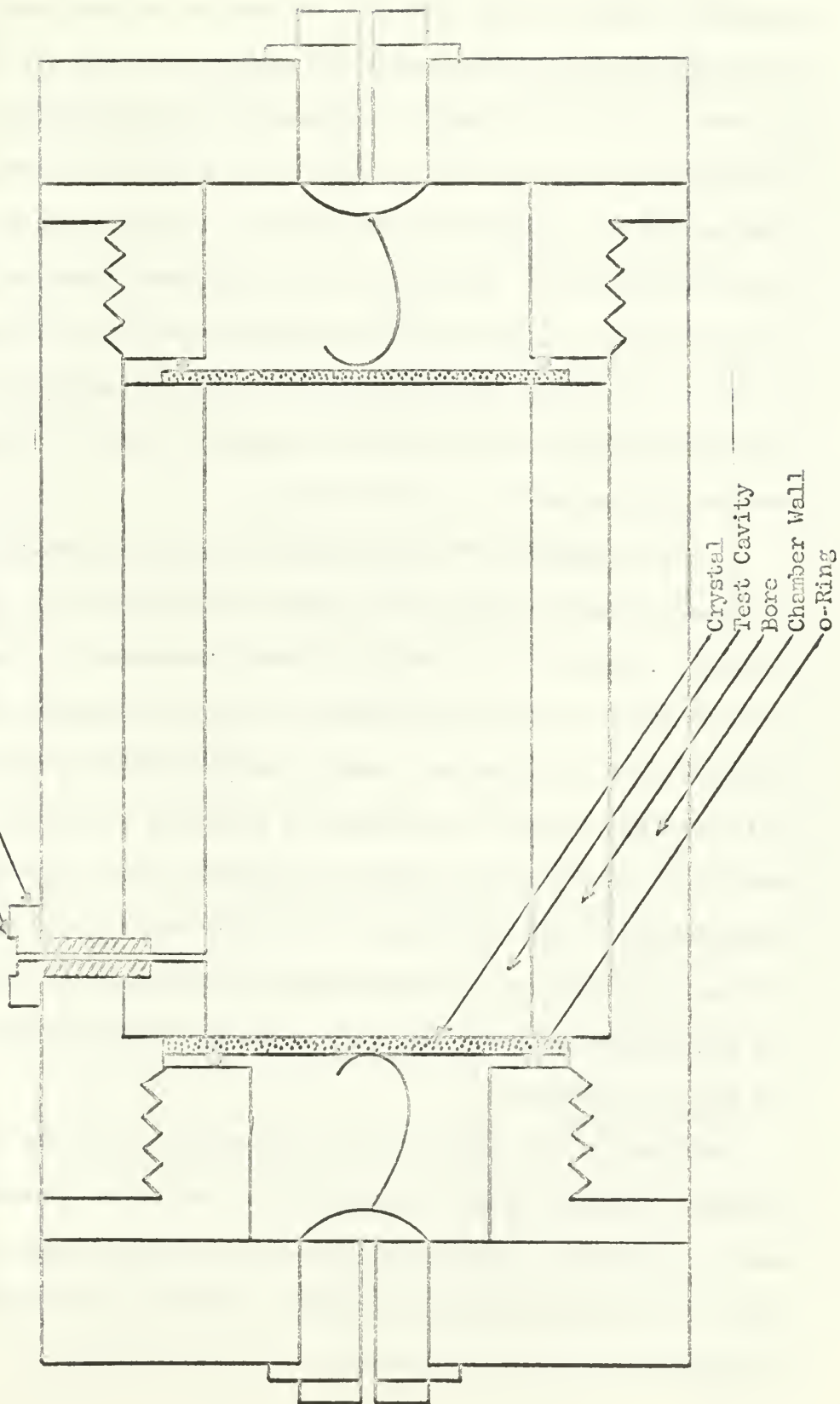


Figure 3. Cutaway Drawing of Acoustical Waveguide.

way transmission is therefore taken to be the distance between the crystals. Rubber O-rings were used to provide an even circular strain on the crystals and vacuum grease was used on the edges of the crystals to ensure liquid tight seals. Low tension spring electrical connectors were used for the electrical contact to the gold plated surface to minimize any force applied to the crystal. Two removable end caps permit easy assembly. The small positioning screw prevents any torsional motion of the bore within the assembly and the filling hold provides a simple way of eliminating air from the cavity and ensuring that fluid completely fills the test chamber, as well as providing a pressure release outlet from the cavity.

A block diagram of the associated electrical equipment necessary for detecting and monitoring the output voltage waveforms is shown in Fig. 4. Table I is a listing of these components by type. The 1.5 volt battery and voltage divider provide a convenient reference voltage on the oscilloscope. When a ten-turn potentiometer was used as the voltage divider it provided the reference voltage of adequate sensitivity necessary for accurate placement in the millivolt range. Determination of the amplitude of any particular pulse within a waveform was accomplished by superimposing the dc reference voltage upon the pulse in question and reading the desired voltage directly from the digital voltmeter.

Although a unit impulse function was desired for the driving voltage, it was, of course, unobtainable. The pulse generator, however, did provide a rectangular pulse of 0.08 microseconds duration, which is less than the time of flight of sound in the crystal of 0.01 microseconds and therefore adequate for this experiment.



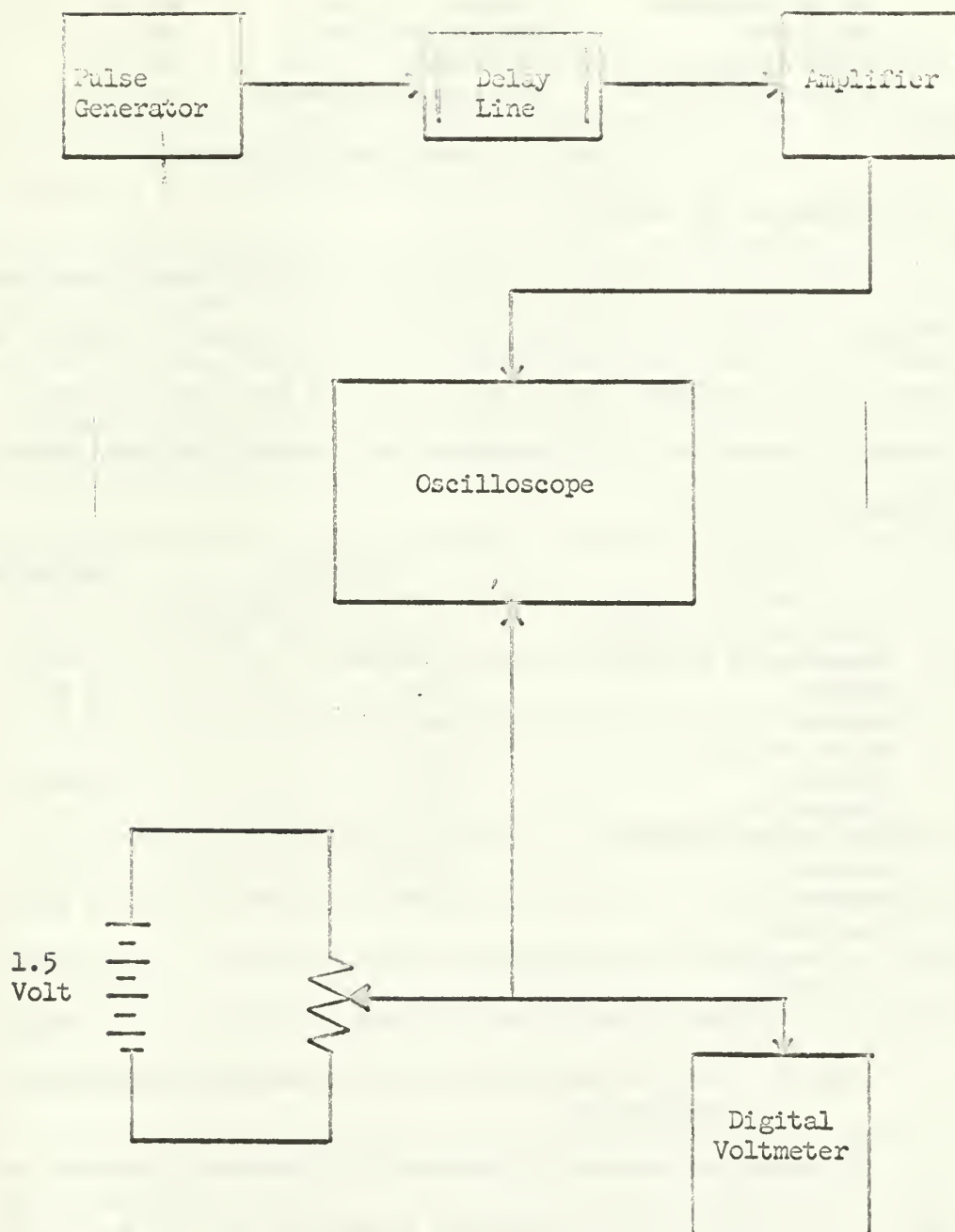


Figure 4. Associated Electrical Equipment.

EQUIPMENT	MANUFACTURER	MODEL
Pulse Generator	DuMont	404 B
Amplifier	Hewlett Packard	460 A
Oscilloscope	Fairchild	766 H
Digital Voltmeter	Electric Instruments	DXA-000

TABLE I. ASSOCIATED EQUIPMENT.

## 5. Discussion of Results

To test the validity of the theory, distilled water was chosen because it makes an excellent acoustic bond to quartz crystals and because its impedance lies in the region of particular interest. The acoustic impedances of all materials of interest for this report are listed in Table II.

MATERIAL	IMPEDANCE	REFERENCE
Fresh water T = 21°C	$1.48231 \times 10^6$ rayls	6,7
Fresh water T = 25°C	1.49164 "	6,7
Quartz	1.52 "	8
Glycerol	2.50 "	7
Nitro benzine	1.79 "	7
Mercury	19.7 "	9
Turpentine	1.11 "	9
Tert-butyl Chloride	0.827 "	10
Acetone	0.725 "	10
Pentane	0.66 "	8
Sea water		
T = 25°C, S = 34.0 ppt	1.56738 "	6,11
Sea water		
T = 25°C, S = 35.0 ppt	1.57084 "	6,11

TABLE II. Various Materials and their Respective Acoustic Impedances.

The water was carefully degassed by alternately heating and applying a vacuum. The temperature stabilized at 21°C prior to testing. The driving voltage  $V(t)$  was a rectangular pulse of duration 0.08 microseconds and of amplitude 30 volts.

The first five voltage waveforms  $E_1^0$  through  $E_5^8$  were photographed and the first two,  $E_1^0$  and  $E_2^8$ , were carefully analyzed for the amplitude of each individual pulse within the waveform. Values



for these individual pulse amplitudes for  $E_1^o$  are listed in Appendix II, and for  $E_1^a$  in Appendix III.

With the help of the computer program previously mentioned, theoretical output voltages were computed and graphed. The computed amplitudes of the individual pulses within  $E_1^o$  and  $E_1^a$  are also listed in Appendices II and III. It should be noted that these computed amplitudes do not include the constant  $kRLo^2/\rho c$  from Eqs. 12 and 30, and are computed for a driving voltage given by an impulse function of unit height. In addition, the measured voltages listed were corrected for the constant amplification factor caused by the wide band amplifier. The calculated voltages do include the correction for the amplitude of the driving voltage which was 30.0 volts vice 1.0 volt. The columns in Appendices II and III labeled "Calculated Voltages and Measured Voltages" should therefore be used for comparison.

The computed voltages  $E_1^o$  through  $E_1^8$  for distilled water are shown in Figs. 5 through 9. The photographs of the actual voltage waveforms  $E_1^o$  through  $E_1^8$  are shown in Figs. 10 through 14. These figures show that there is excellent agreement between theory and measurement.

For comparison, Fig. 15 is a plot of the envelopes of the actual and calculated voltages for the first received output,  $E_1^o$ . The solid curve represents the calculated envelope and the dots represent actual measured pulses. Fig. 16 is the same plotted data for the second received output  $E_1^a$ . Since the relative shapes of the waveform are of particular interest, rather than the absolute amplitudes, the actual values have been normalized so that the maximum positive voltages, measured and calculated, coincide.

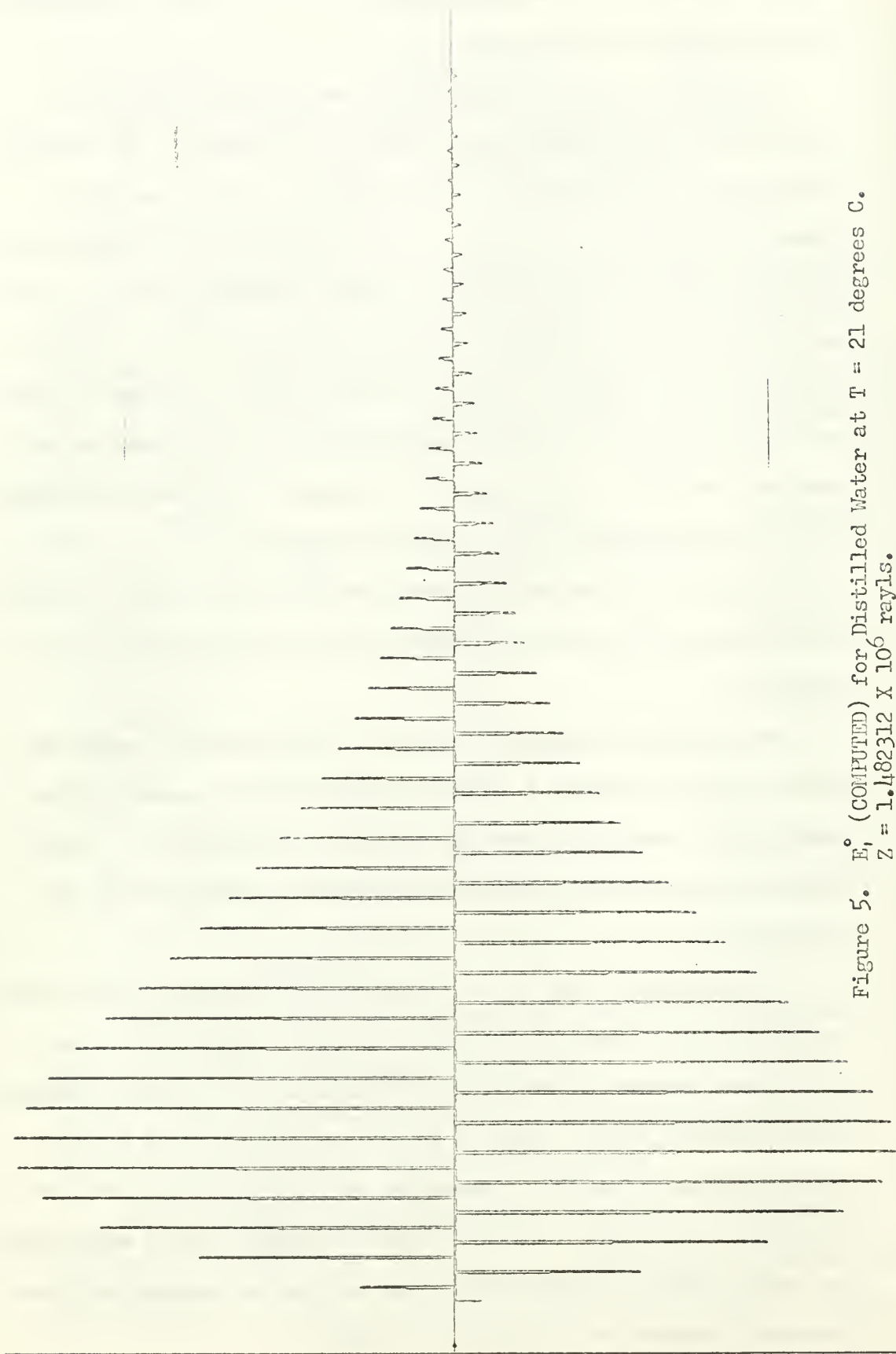


Figure 5.  $E_z$  (COMPUTED) for Distilled Water at  $T = 21$  degrees C.  
 $Z = 1.482312 \times 10^6$  rayls.  
 Time between pulses is 0.1 microseconds.

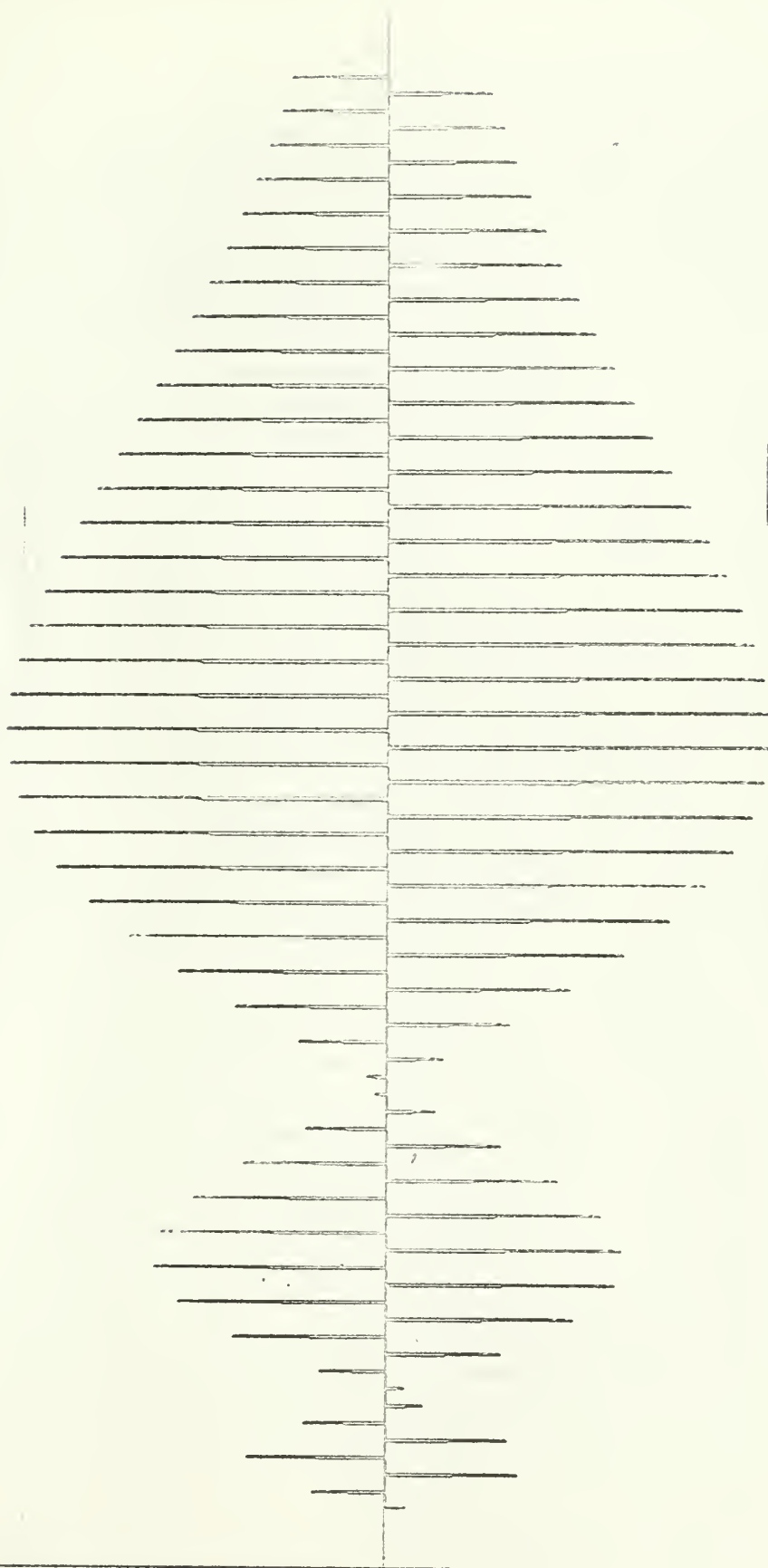


Figure 6.  $E_1^2$  (COMPUTED) for Distilled Water at  $T = 21$  degrees C.  
 $Z = 1.482312 \times 10^6$  rayls.  
 Time between pulses is 0.1 microseconds.

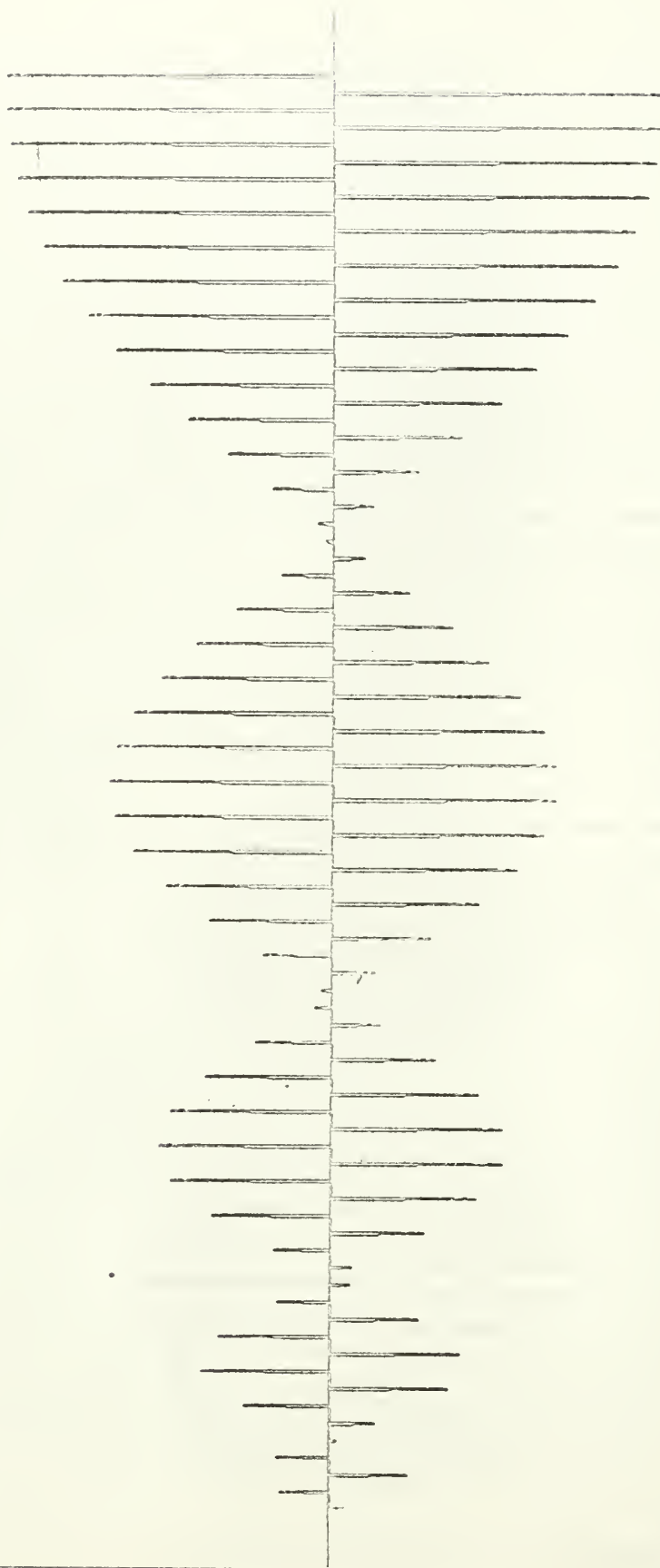


Figure 7.  $E^*$  (COMPUTED) for Distilled Water at  $T = 21$  degrees C.  
 $Z = 1.482312 \times 10^6$  rays.  
Time between pulses is 0.1 microseconds.

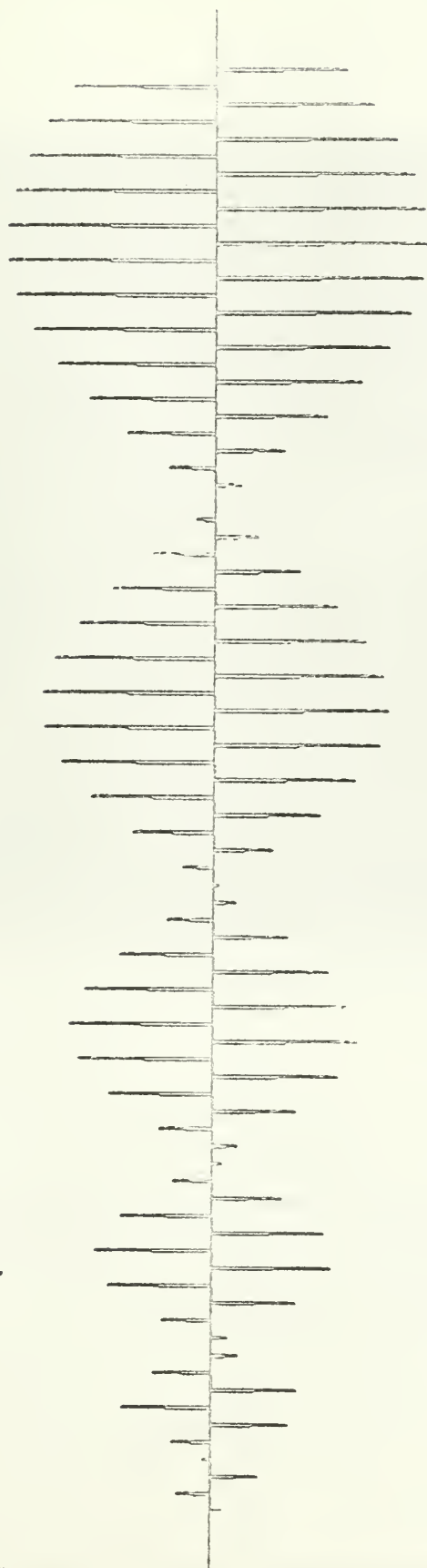


Figure 8.  $E'$  (COMPUTED) for Distilled Water at  $T = 21$  degrees C.  
 $Z = 1.482312 \times 10^6$  rayls.  
Time between pulses is 0.1 microseconds.

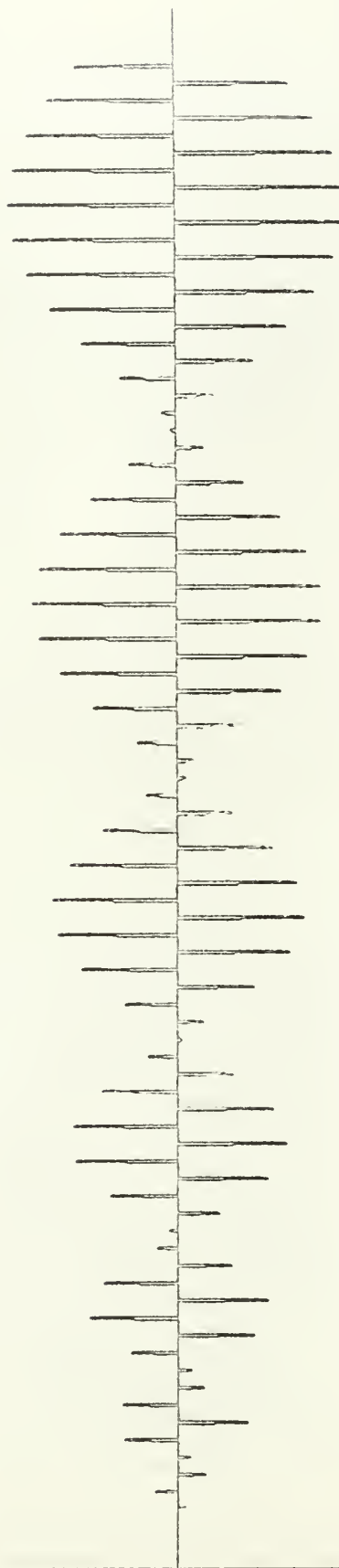


Figure 9.  $E''$  (COMPUTED) for Distilled Water at  $T = 21$  degrees C.  
 $Z = 1.482312 \times 10^6$  rayls.  
Time between pulses is 0.1 microseconds.

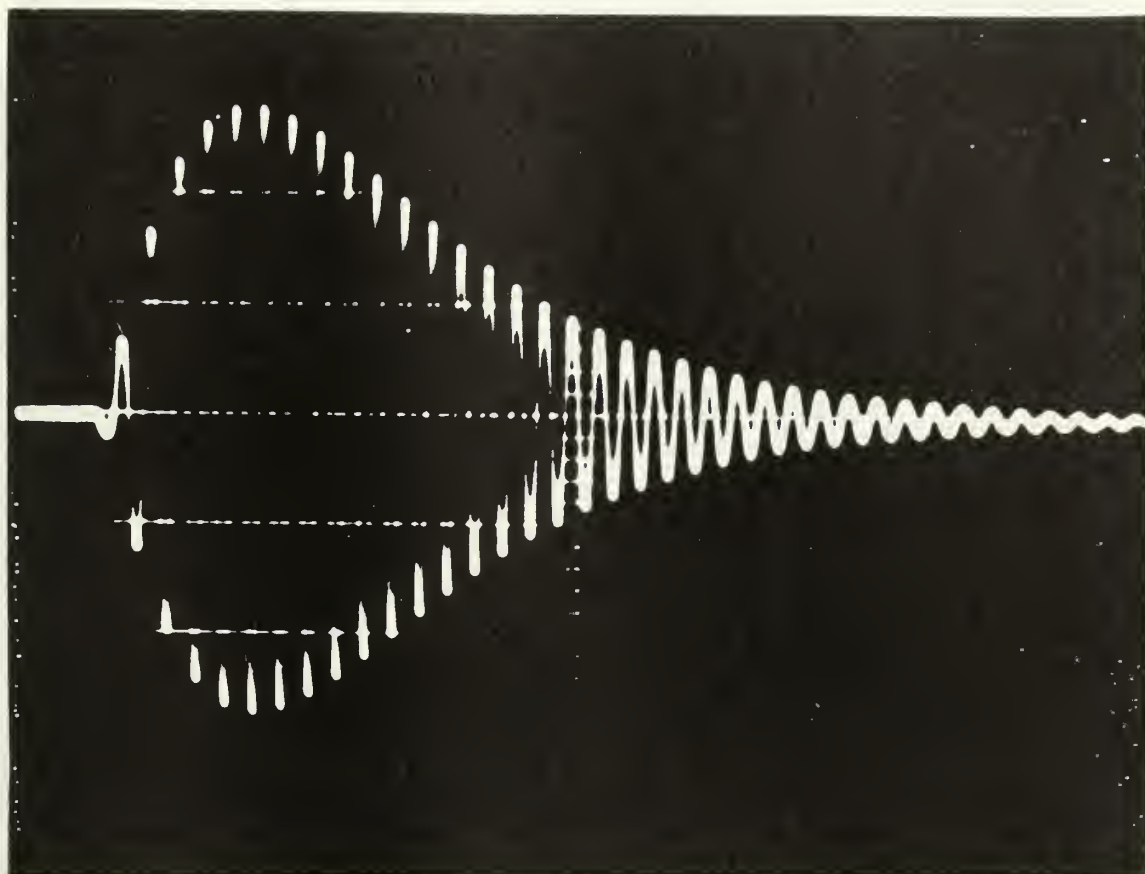


Figure 10. Photograph of the waveform  $E_1^O$  for distilled water at  $T=21$  degrees C.



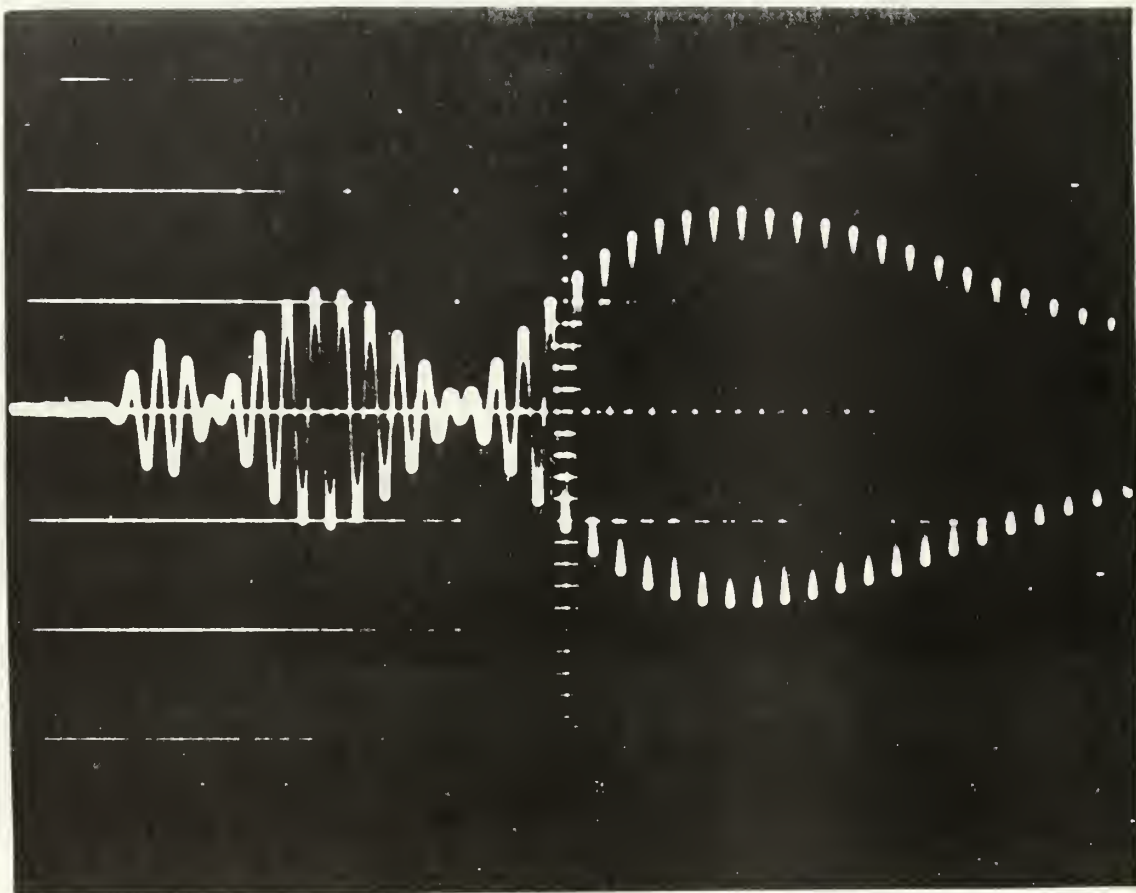


Figure 11. Photograph of the waveform  $\alpha_1^2$  for distilled water at  $T=21$  degrees C.



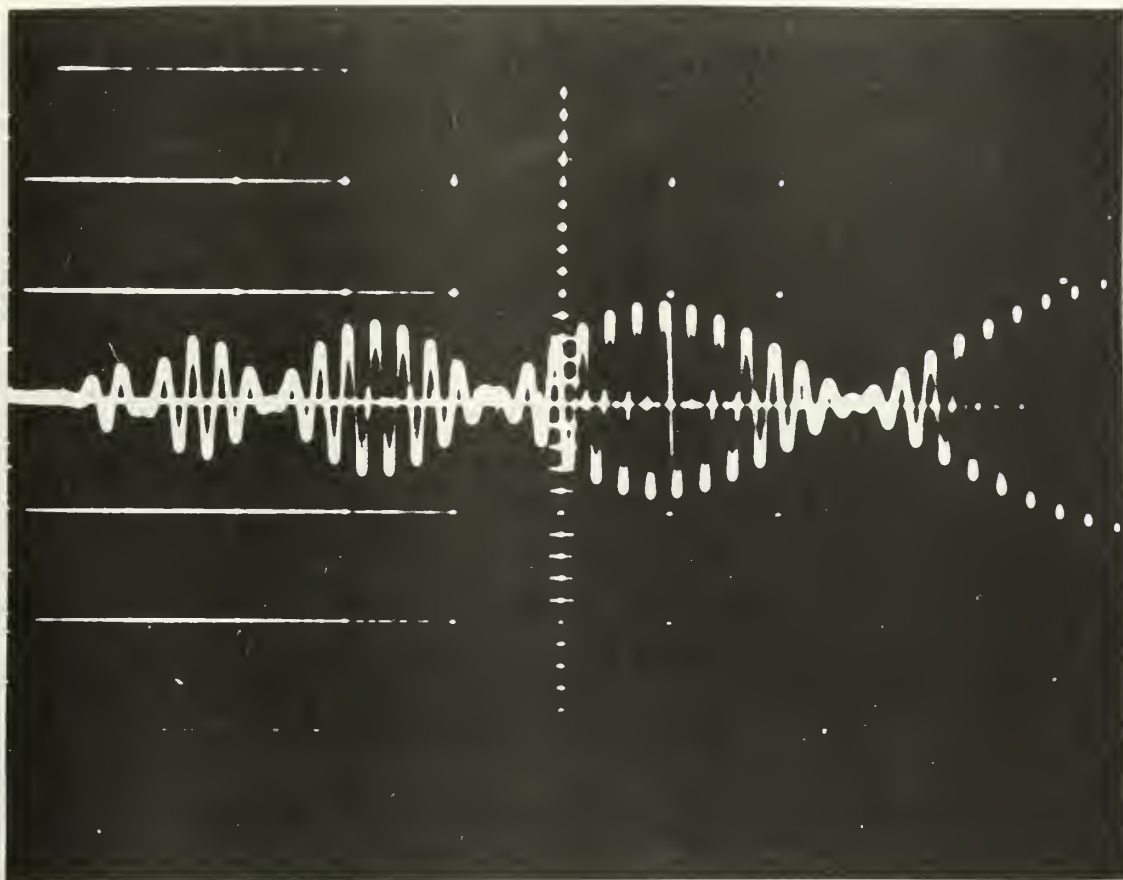


Figure 12. Photograph of the waveform  $E_1^*$  for distilled water at  $T=21$  degrees C.

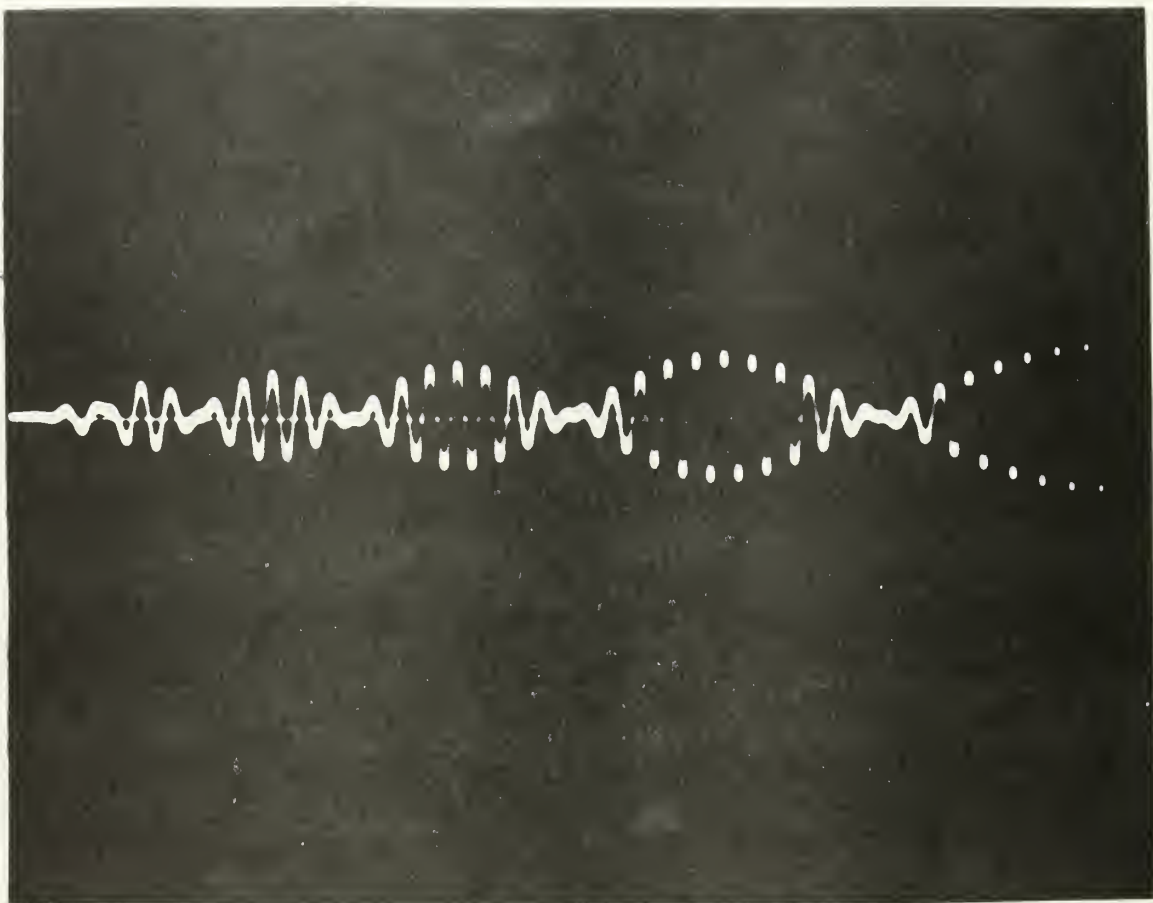


Figure 13. Photograph of the waveform  $E_1^6$  for distilled water at  $T=21$  degrees C.

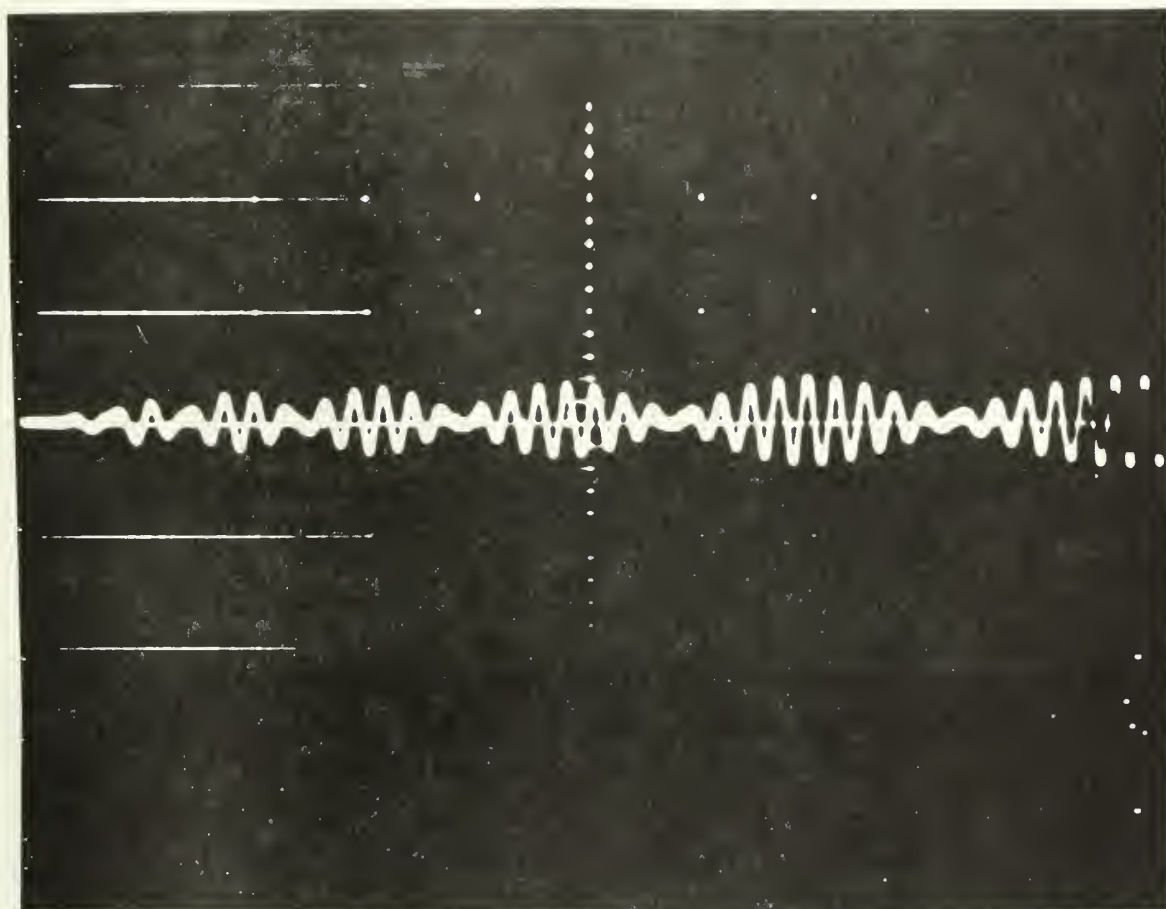


Figure 14. Photograph of the waveform  $E_1^B$  for distilled water at  $T=21$  degrees C.

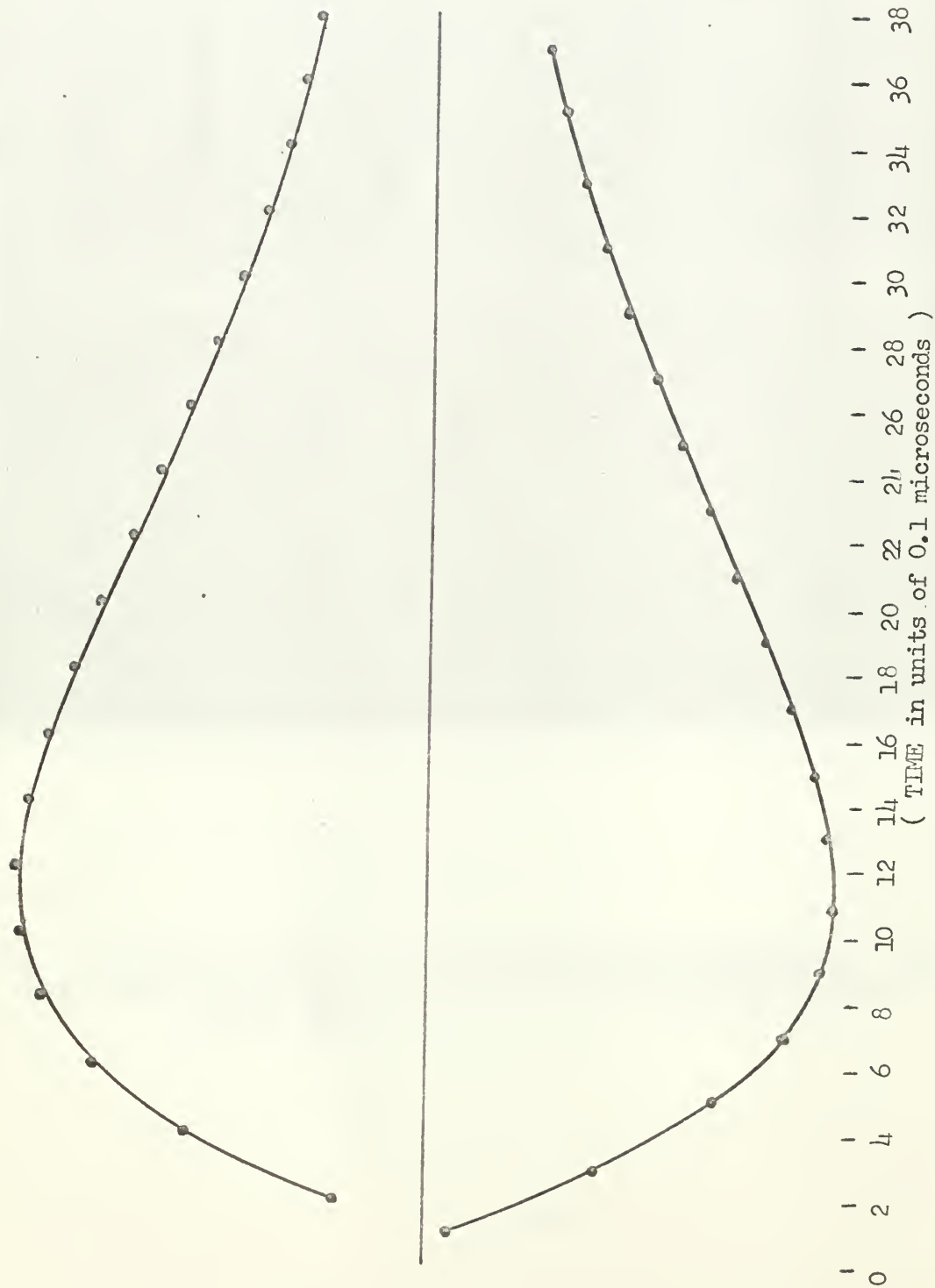


Figure 15.  $E_0$  for Distilled Water.  $T=21^\circ\text{C}$  (  $Z=1.482312 \times 10^6$  rays )  
 Solid curve represents theoretical envelope.  
 Dots represent normalized experimental data.

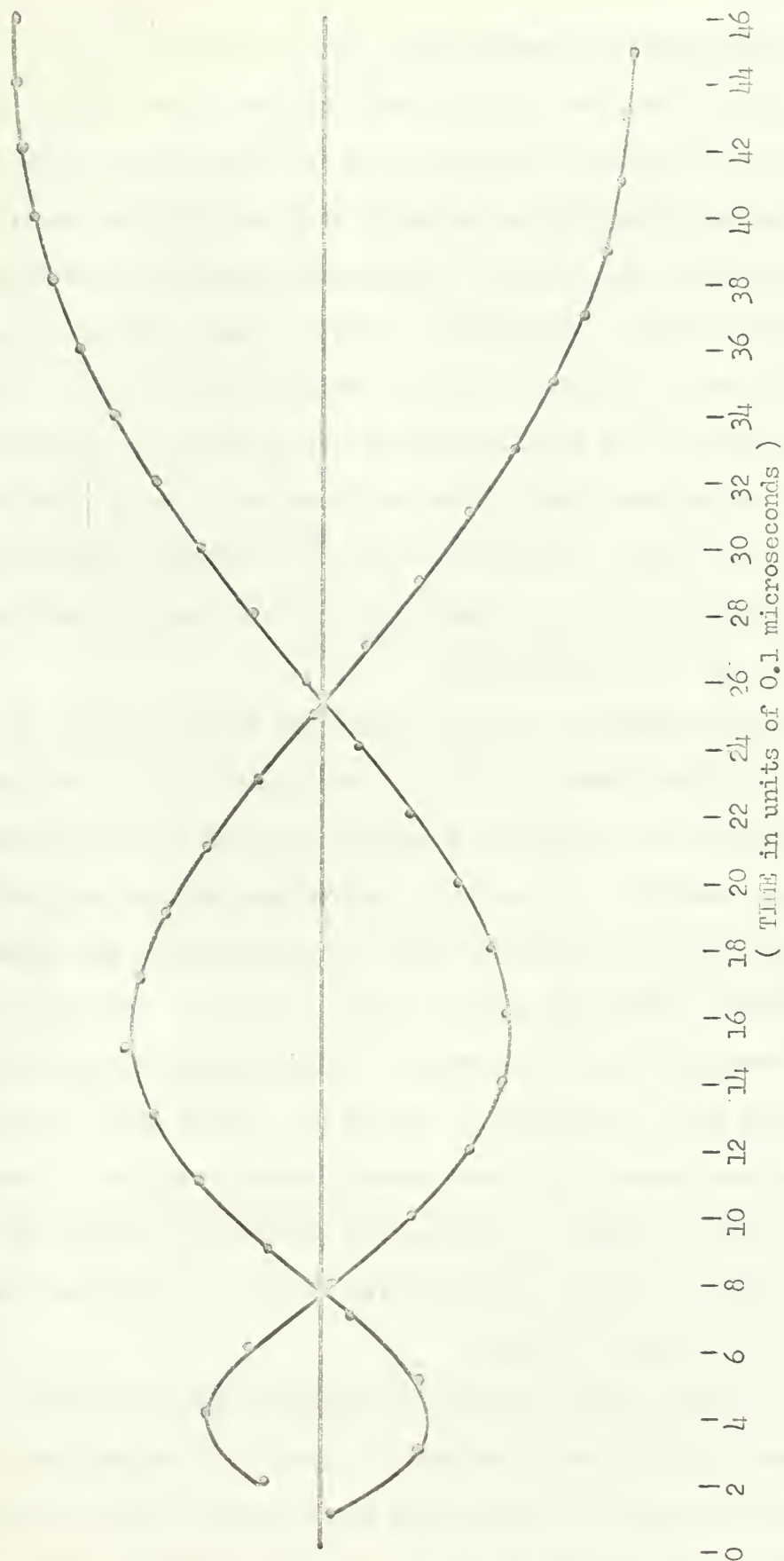


Figure 16.  $E_1^2$  for Distilled Water.  $T=21^\circ\text{C}$  ( $Z=1.482312 \times 10^6$  rays) —

Solid curve represents theoretical envelope.

Dots represent normalized experimental data.

It was observed that each actual negative pulse fell farther from the calculated curve than did each positive pulse. This suggested that the dc reference voltage on the oscilloscope was slightly biased; further investigation indicated that the wide band amplifier was not symmetric, ie., positive pulses were amplified slightly more than negative pulses. Consequently, just the amplitudes of the positive pulses were recorded. Since the maximum reading error of the voltage pulses was the error associated with placing the dc reference on top of the voltage trace on the oscilloscope, it was a fixed error for all pulses. This fixed positioning error therefore, causes much larger maximum possible percentage errors for the smaller amplitude pulses than for the larger pulses.

With the exception of the salt water and distilled water at 25.0°C, the fluids listed in Table II were tested in this analysis. The absorption was so great for glycerol that only the first output voltage was received. The acoustic bond between mercury and quartz was so poor that only the first output voltage waveform was assumed to be reliable. These are shown in Figs. 22 and 23. The results for pentane, tert-butyl chloride, acetone, turpentine and nitro-benzene are shown in Figs. 17 through 21. As in the case of water, the individual voltage pulses within each waveform were normalized to the maximum positive voltage to indicate the correlation in waveform shapes between the actual and calculated values. As mentioned above, only positive values are shown.

In all cases, prior to testing the known fluid, the crystals were cleaned with potassium hydroxide to remove the vacuum grease that may have coated the crystal from prior testing. This, however, was the only special precaution taken. The test fluids were taken

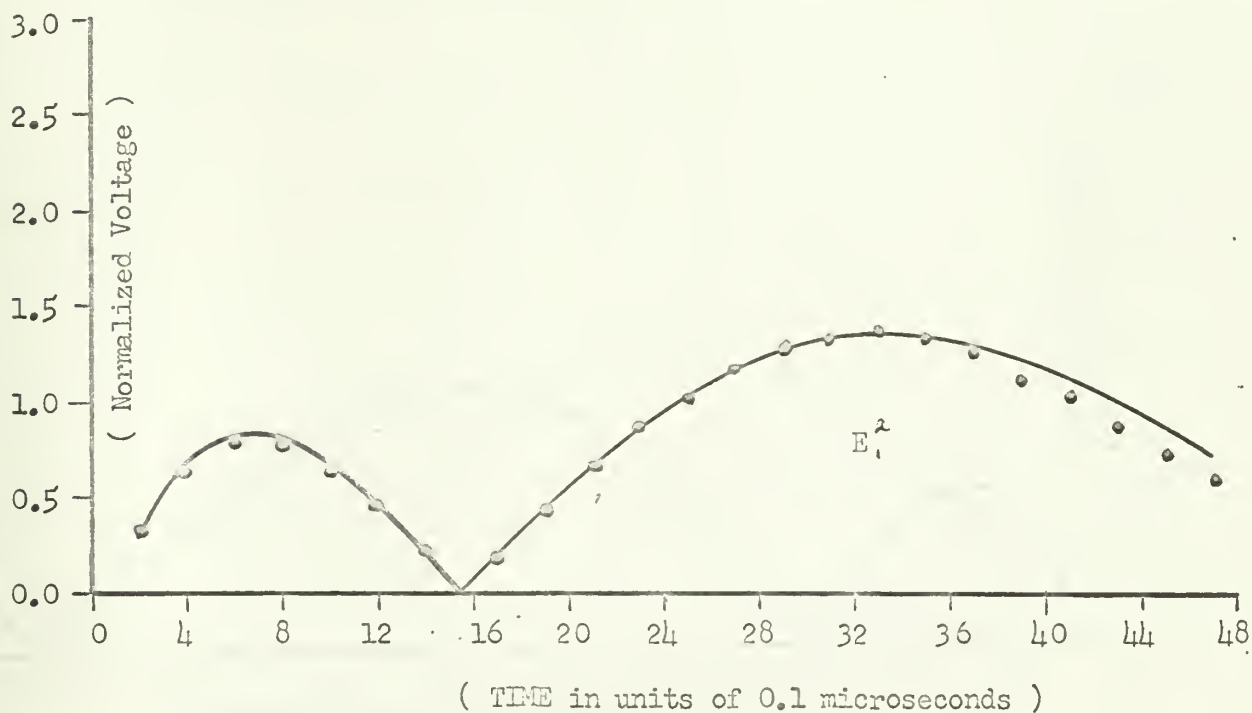


Figure 17.  $E_1^0$  and  $E_1^2$  for Pentane. (  $Z=0.66 \times 10^6$  rayls )  
Solid curve represents theoretical envelope.  
Dots represent normalized experimental data.



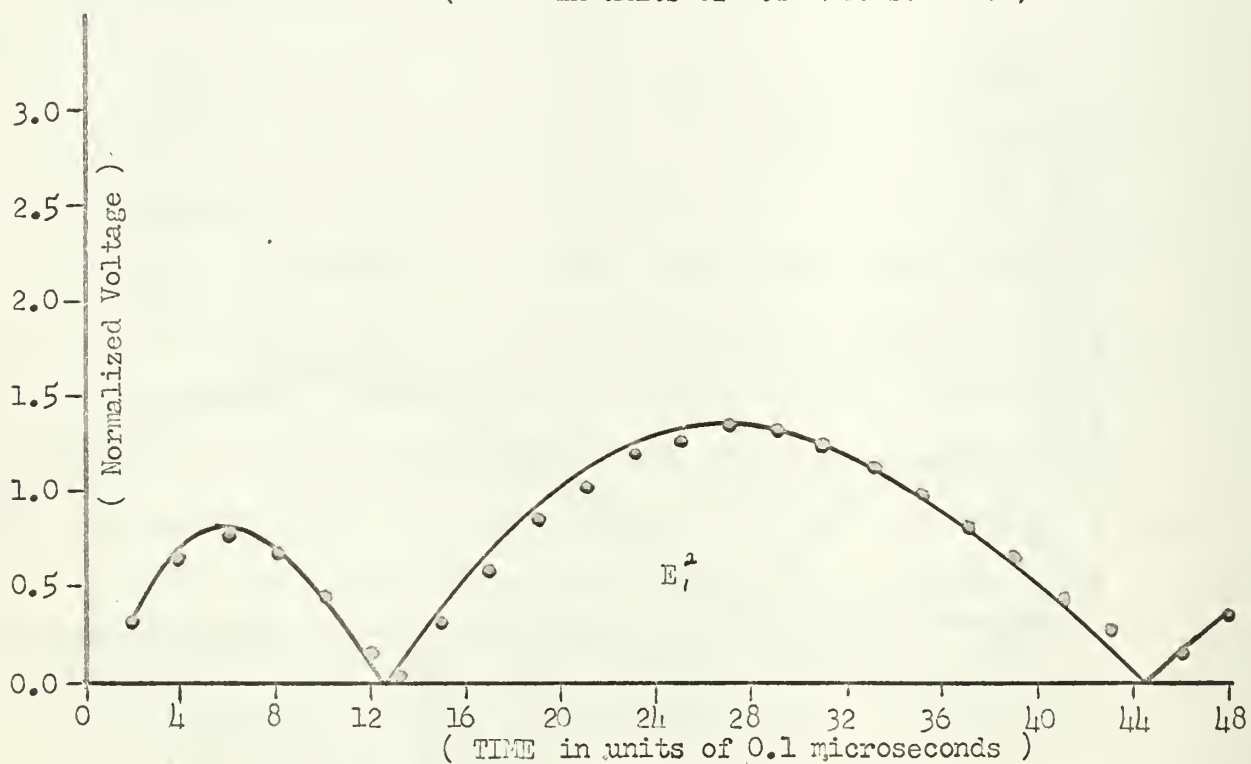
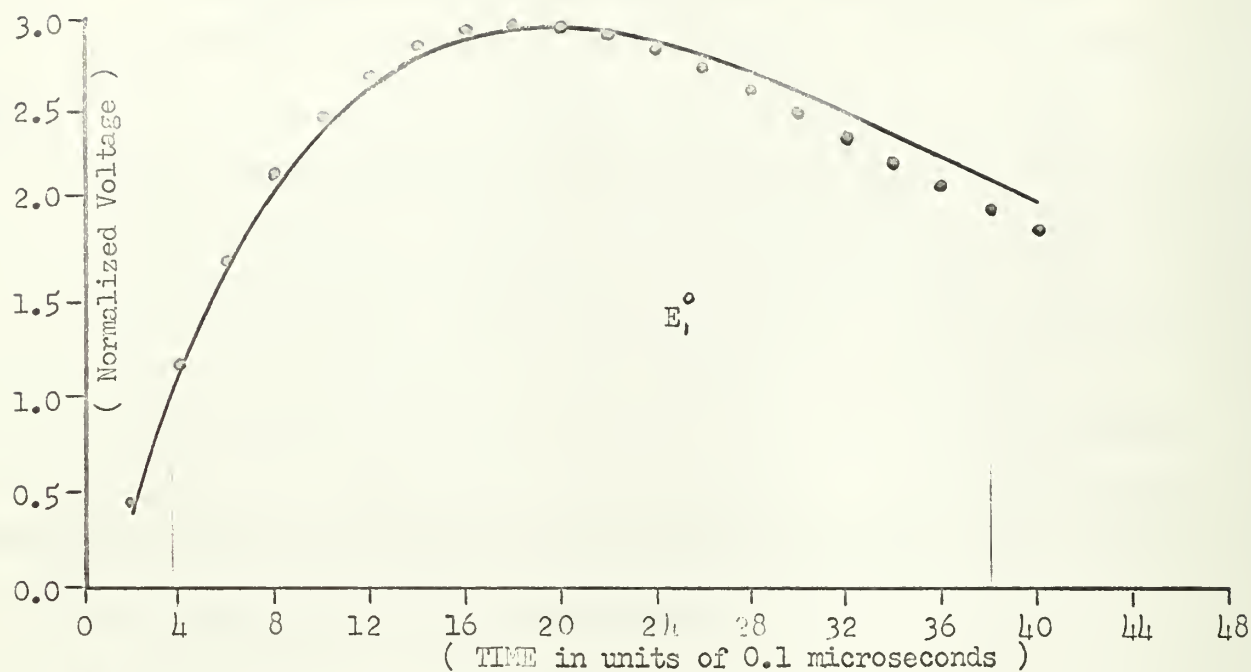


Figure 18.  $E_1^0$  and  $E_1^2$  for Tert-Butyl Chloride. (  $Z=0.827 \times 10^6$  rayls )  
 Solid curve represents theoretical envelope.  
 Dots represent normalized experimental data.

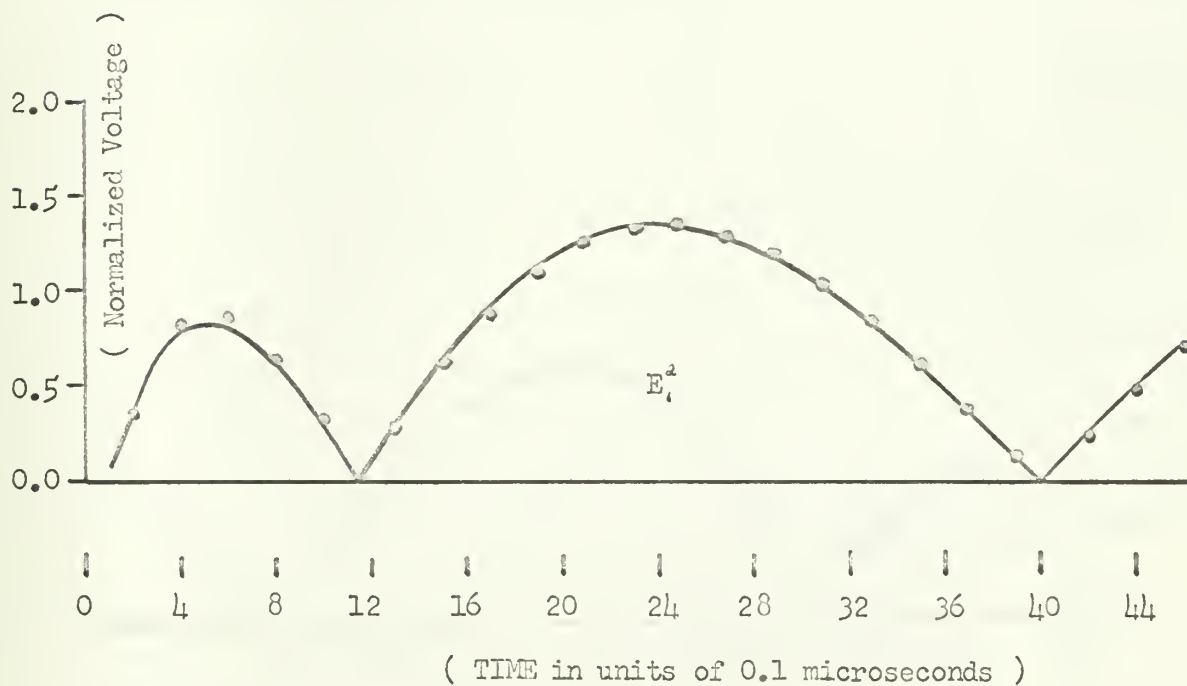


Figure 19.  $E_c$  and  $E_c^2$  for Acetone. (  $Z=0.925 \times 10^6$  rayls )  
 Solid curve represents theoretical envelope.  
 Dots represent normalized experimental data.

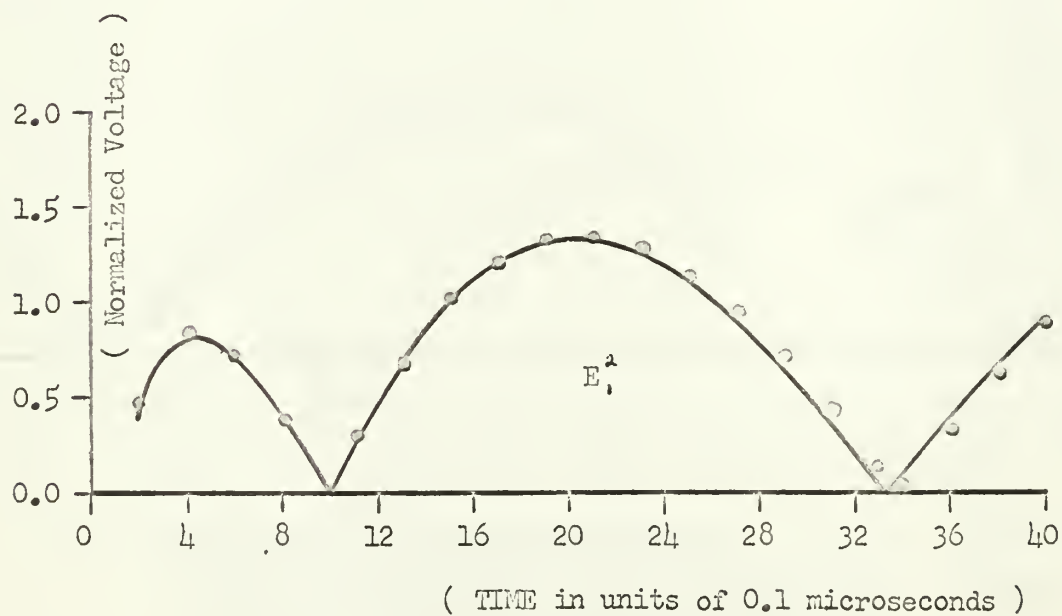
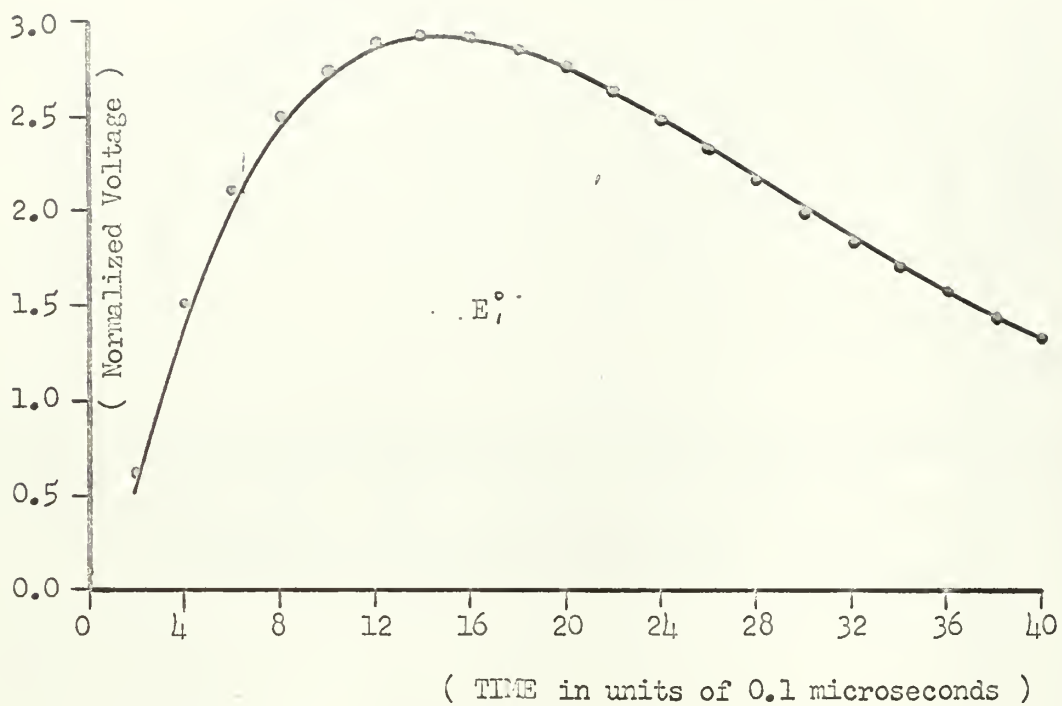


Figure 20.  $E_1^0$  and  $E_1^2$  for Turpentine. ( $Z=1.11 \times 10^6$  rayls)  
 Solid curve represents theoretical envelope.  
 Dots represent normalized experimental data.

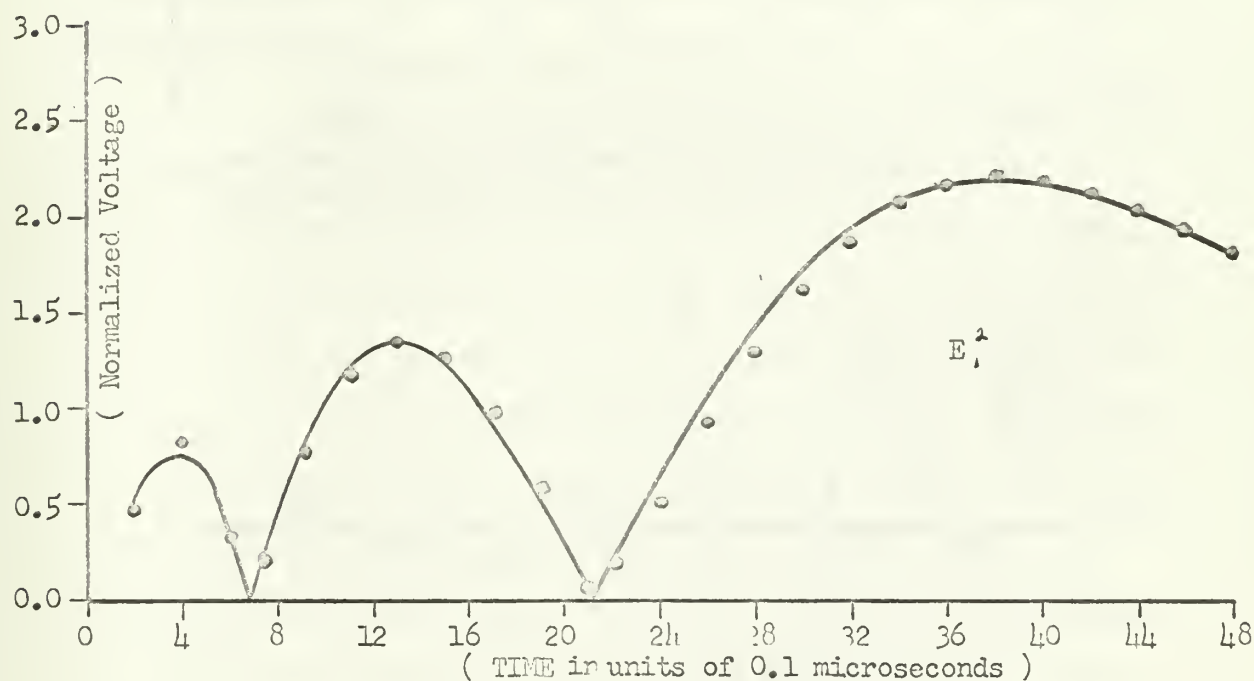
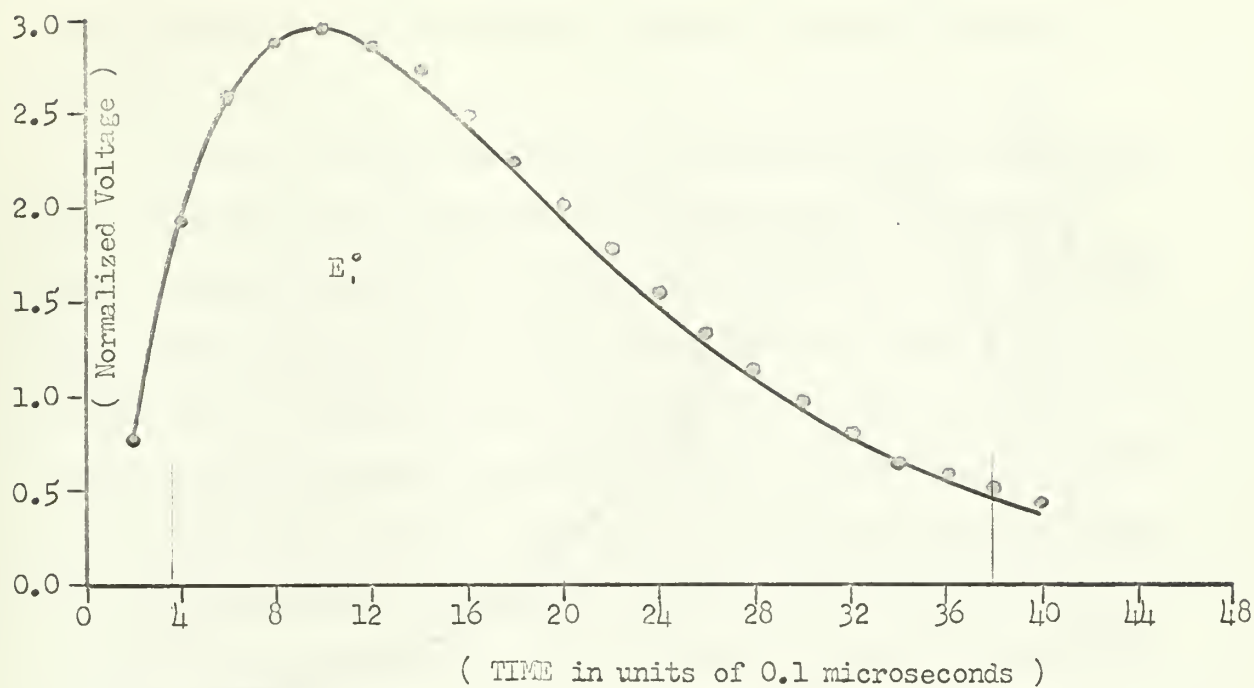


Figure 21.  $E_0$  and  $E_1^2$  for Nitro Benzene. (  $Z=1.788 \times 10^6$  rayls )  
 Solid curve represents theoretical envelope.  
 Dots represent normalized experimental data.

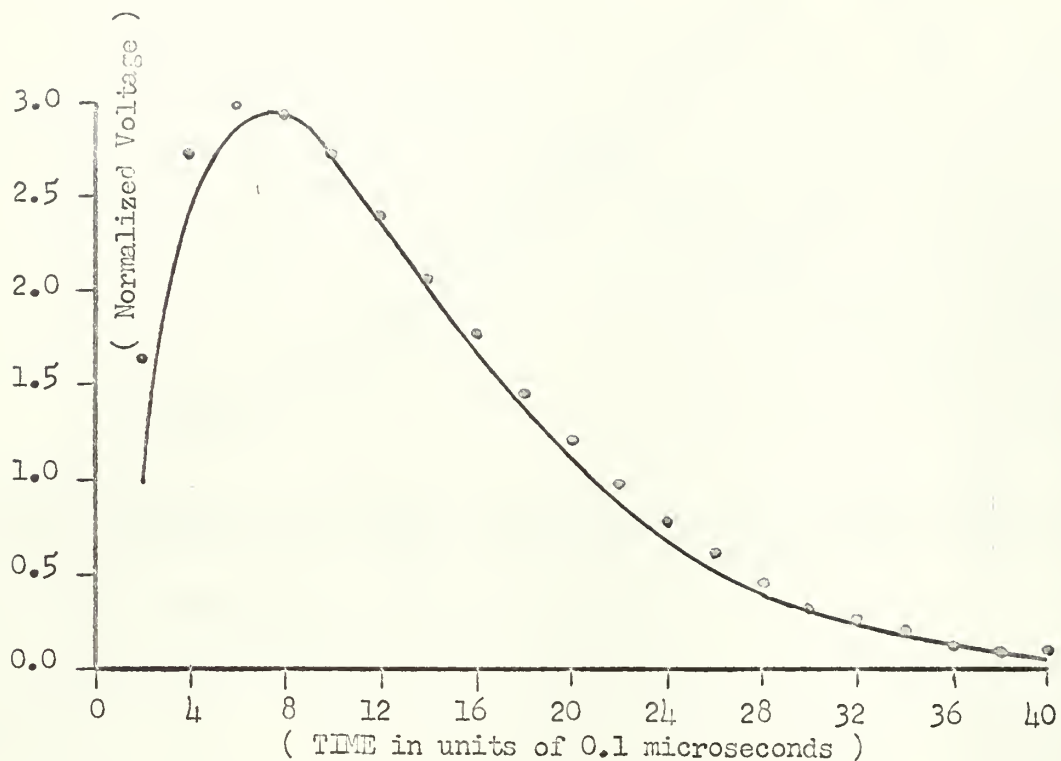


Figure 22.  $E_1^0$  for Glycerol. ( $Z=2.50 \times 10^6$  rayls.)  
Solid curve represents theoretical envelope.  
Dots represent normalized experimental data.

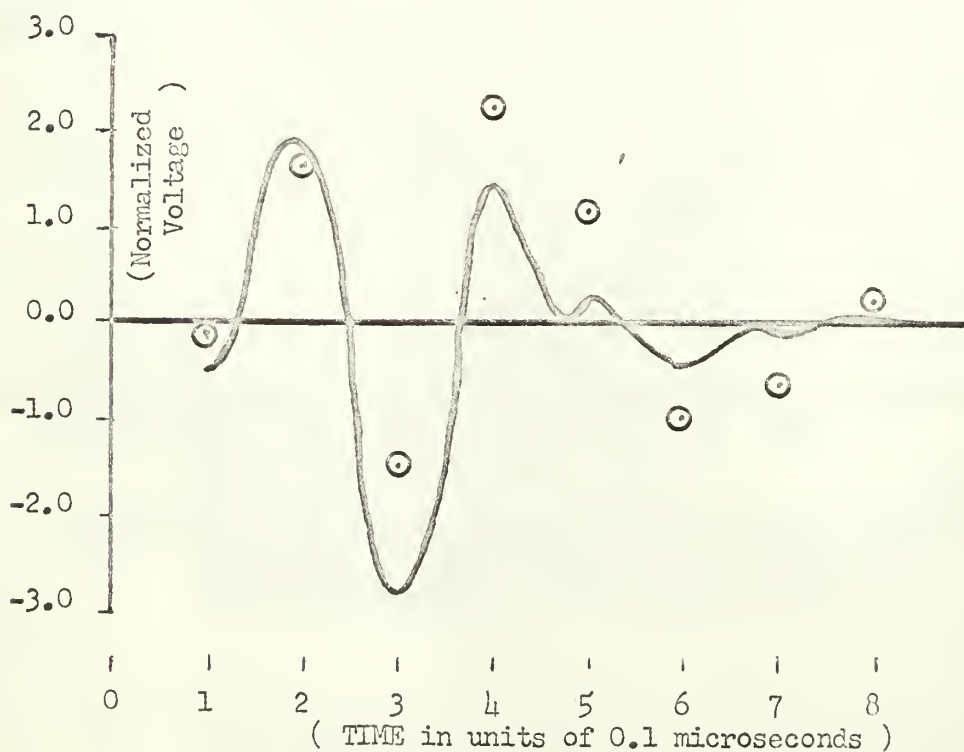


Figure 23.  $E_1^0$  for Mercury. ( $Z=19.7 \times 10^6$  rayls.)  
Solid curve represents theoretical envelope.  
Dots represent normalized experimental data.

from laboratory supplies and were assumed to have the values of  $\rho c$  listed in Table II.

With the exception of mercury, no difficulties were encountered in obtaining results. Because of the difficulties in obtaining a good acoustic bond between mercury and quartz however, special problems did develop. The unpolished quartz crystals enabled some trapped air to exist between the mercury and the crystal. It was thought that coating the crystal with a thin film of fluid, with an impedance closer to mercury than to air, would fill the spaces in the face of the crystal, permitting a reasonable bond. Liquid soap was finally used as the coating fluid and adequate results then were obtained and are shown in Fig. 23.

## 6. Error Analysis

With the exception of glycerol and mercury, the first two output voltages  $E_1^o$  and  $E_1^a$  are shown for the fluids tested in Figs. 17 through 21. Only the first two are shown because it is felt that these two, and in particular the second, supply sufficient information to confirm the theory and to enable a definite correlation criterion between acoustic impedance and output waveforms. In addition, the assumptions previously mentioned of lossless crystals and fluids, become less valid as the pulses continue to propagate. A few of these neglected losses are; losses within the crystal, absorption in the fluid, beam spreading within the fluid and improper geometrical alignment of crystals and the fluid chamber.

In general, the assumption of lossless crystals will remain valid for all pulses, since the fractional loss within the crystal of each pulse should remain the same for all pulses, regardless of amplitude.[12] Beam spreading should be at a minimum for a perfectly

guided wave, that is, with the plated crystal diameter being exactly equal to the diameter of the test cavity. However, when crystals of smaller plating diameter are used, spreading losses can become significant, [3] eventually causing the amplitude of each pulse to decrease below the predicted values. If the crystals are not parallel, the wave front will strike the crystal at an angle slightly different from the normal, causing a decrease in amplitude. As previously mentioned, care was taken in the equipment design and construction to minimize this error.

Although the absolute values of the individual pulses have not been considered in this study, a knowledge of the ability to predict their values is necessary as a further confirmation of the theory: Equation 30 can be expressed as

$$E = - \frac{h R C_0}{Z} \frac{T_1}{M_1} F(p) \quad (31)$$

where  $F(p)$  is the infinite series of pressure terms. Equation 12, however, enables us to write the pressures as a function of applied voltages. Therefore Eq. 31 becomes

$$E = - \frac{h R C_0}{Z} \frac{T_1}{M_1} F(a v_{e1}), \quad (32)$$

$$\text{or } E = - \frac{h R C_0}{Z} a \frac{T_1}{M_1} F(v),$$

and  $\frac{T_1}{M_1} F(v)$  is what the program listed in Appendix I is designed to compute. By defining

$$X = \frac{T_1}{M_1} F(v),$$

Eq. 31 may be expressed as

$$E = - \frac{h R C_0}{Z} a X \quad (33)$$

from Eq. 4,  $a = \epsilon \frac{h}{4\pi d}$ , therefore

$$E = - \frac{h^2 R C_0 \epsilon}{4\pi d Z} X \quad (34)$$



The rms uncertainty in E may therefore be expressed as

$$\frac{dE}{E} = \left[ 2\left(\frac{dZ}{Z}\right)^2 + \left(\frac{dR}{R}\right)^2 + \left(\frac{d\epsilon}{\epsilon}\right)^2 + \left(\frac{dd}{d}\right)^2 + \left(\frac{dZ}{Z}\right)^2 + \left(\frac{dX}{X}\right)^2 \right]^{1/2} \quad (35)$$

where  $\frac{df}{f}$  designates the uncertainty in the quantity f.

From repeated calculations using the computer program it can be shown that variations in either Z, Z<sub>1</sub>, or Z<sub>2</sub> of up to 10 percent causes an amplitude deviation in X of less than 0.1 percent. However, variations in the applied voltage have a direct bearing on the output voltage and the input voltage is estimated to be accurate to well within 1.0 percent. The overall change in the output voltage due to the error in X is therefore, estimated to be 1.0 percent or less.

From Bechman,[13] h is  $(43.6 \pm 0.1) \times 10^8$  v/m and  $\epsilon$  is  $(4.32 \pm 0.01)\epsilon_0$  farads/m. From Mason,[8] the acoustic impedance of quartz, Z, is  $(1.52 \pm 0.01) \times 10^6$  rayls. The equipment manual listed R as 200 ohms and its accuracy was estimated to be 5.0 percent. The value of C<sub>0</sub> was measured as  $80 \times 10^{-6}$  farads, with an estimated accuracy of 10.0 percent. d was measured as 0.0226 inches with an accuracy 0.0001 inches. Substitution of the above possible values into Eq. 35 yields a maximum possible error in the prediction of the output voltages of 12 percent. The percentage difference between theoretical and actual voltage for any particular pulse within E<sub>i</sub><sup>o</sup>, for distilled water at 21.0 degrees C., is less than 6 percent, well within the maximum possible of 12 percent.

## 7. Data Evaluation and Conclusions

Examination of the output voltages E<sub>i</sub><sup>o</sup> and E<sub>i</sub><sup>a</sup> for all of the computed waveforms indicates that the impedance of the fluid in question cannot accurately be determined from the first voltage waveform.

The second voltage  $E_1^2$ , however, shows two distinct points of interest. Successive reflections from the faces of the crystals causes an interaction of pulses within the waveform which results in a modulated output voltage. Within the second output voltage waveform  $E_1^2$ , there are two points where the envelope of the modulated voltage goes to zero.

When a comparison of the second output waveforms was made for the various test fluids, it was noted that as the acoustic impedance increased, the waveforms appear to be compressed, causing the points of zero amplitude, or points at which the change of phase occurs to be pushed forward in time. The relationship between these phase changes and the impedance of the fluid in the waveguide can be seen in Fig. 24. Figure 24 is a plot of the acoustic impedance as the ordinate, and the time to reach the first and second axis crossing as the abscissa. The ordinate represents the entire range of impedances studied where the axis crossings are discernable. Values of the various impedances used as well as the theoretical and actual values of time for the first and second axis crossing are listed in Table 11.

Figures 25 and 26 are expanded sections of Fig. 24 for the range of impedance of particular interest. The solid curve represents the calculated values and the dots are the measured values for the fluids investigated. The estimated accuracy for the measured time of axis crossings is 0.1 units. In the neighborhood of water,  $Z = 1.5 \times 10^6$  rayls, the slope of the curve in Fig. 26 is  $0.07 \times 10^6$  rayls per unit abscissa. In this area then, the  $\pm 0.1$  estimated error in axis crossing corresponds to 0.9 percent error in acoustic impedance. The error in impedance measurement near  $2.5 \times 10^6$  rayls

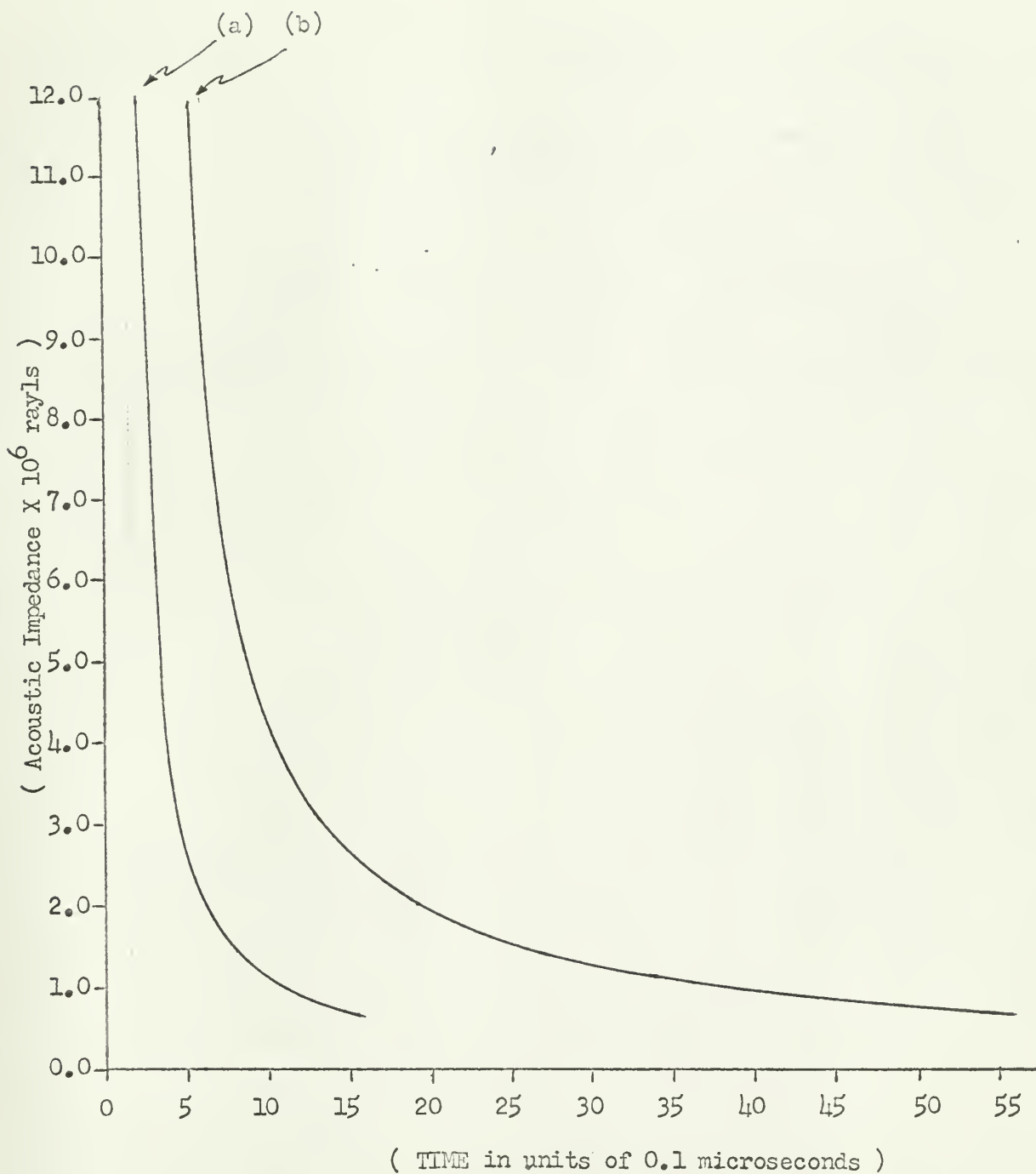
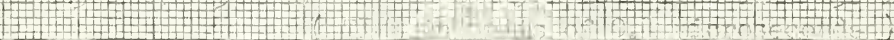
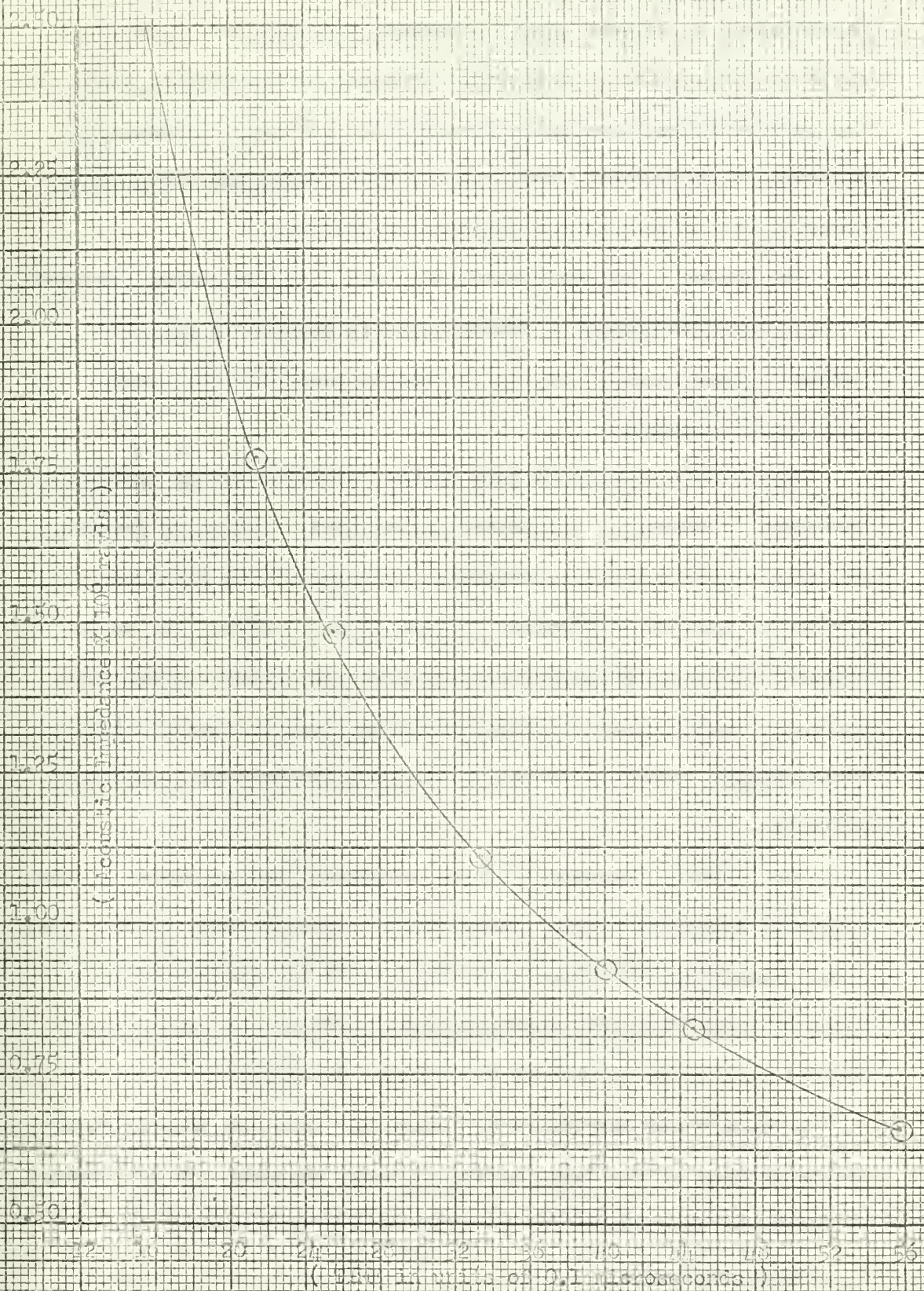


Figure 24. Acoustic Impedance vs. Time to a) First axis crossing.  
b) Second axis crossing.









(Data in units of 0.1 microseconds.)

Figure 2. Acoustic impedance vs. frequency.



is estimated to be less than 2.0 percent and when near  $0.66 \times 10^6$  rays to be less than 0.5 percent. Because of the greater slope of the curve for the first axis crossing, the accuracy of impedance measurement is somewhat less, and for this reason the second axis crossing is recommended for impedance measurements.

The accuracy just mentioned indicates that the method described is not sensitive enough to determine small changes in salinity. Larger changes in salinity, in the neighborhood of 2 to 3 ppt, should be discernable.

Since the most tedious part of the determination of acoustical impedance is measuring all pulses in the area of the axis crossing, and then plotting these to determine the time of the axis crossing, any device that would simplify this would be an asset. If an envelope detector were devised for use with the output voltage waveforms, so that the axis crossing could be directly measured from the oscilloscope, immediate acoustic impedance measurements would be available.

The "carrier frequency" of the output voltage waveforms is the resonance frequency of the piezoelectric crystals used, in this case 5 mc. Since this frequency is within one of the special broadcast bands utilized for radio communications, perhaps the same form of demodulation could be used as an envelope detector.

A "Record and Disclosure of Invention" form has been filed with the Department of the Navy, Office of Naval Research, on this method of impedance measurement for possible Patent Application.

#### 8. Acknowledgements

This work has been supported in part by the U.S. Office of Naval Research, and the U.S. Navy Bureau of Ships. The author would like

to express his appreciation to Asst. Prof. A.B. Coppens for his suggestions and helpful comments, and to Mr. R.C. Moeller and Mr. H.D. Whitfill for their assistance in construction and design of the necessary equipment.



## BIBLIOGRAPHY

1. M. Redwood, "Experiments with the electrical analog of a piezoelectric transducer," J. Acoust. Soc. Am. 36, 1872 (1964).
2. E. G. Cook, "Transient and steady-state response of ultrasonic piezoelectric transducers," IRE Convention Records 9, 61 (1956).
3. H. B. Huntington, A. G. Emslie and V.W. Huges, "Ultrasonic delay lines," J. Franklin Inst. 245, 1 (1948).
4. A. B. Coppens, "An experimental determination of the parameters of nonlinearity,  $B/A$ , in four liquid metals," (Doctorate Thesis, Brown U., 1965).
5. E. J. Craig, Laplace and Fourier transforms for electrical engineers (Holt, Rinehart and Winston, 1964).
6. W. D. Wilson, "Ultrasonic measurement of the velocity of sound in distilled water and sea water," NAVORD Report 6746, (Apr. 1960).
7. American Institute of Physics Handbook (McGraw Hill Book Co. Inc., New York, Toronto and London, 1957).
8. W. P. Mason, Physical Acoustics (Academic Press, New York and London, 1964), Vol. 1 A.
9. L. E. Kinsler and A. R. Frey, Fundamentals of Acoustics (John Wiley and Sons Inc., New York, London, 1962).
10. G. W. Willard, "Ultrasonic absorption and velocity measurements in numerous liquids," J. Acoust. Soc. Am. 13, 438 (1941).
11. E. C. LaFond, Processing Oceanographic Data, H.O. Pub. No. 614 (U.S.N. Hydrographic Office, Wash. D.C., 1951).
12. W. G. Cady, "Measurement of the specific acoustic resistance of liquids," O.N.R. Tech. Report No. 4 (1949).
13. R. Bechman, "Elastic and piezoelectric constants of alfa quartz," Phys. Rev. 110, 1060 (1958).

# APPENDIX I

```

C THE FOLLOWING PROGRAM WILL COMPUTE, PRINT AND PLOT THE VOLTAGE
C OUTPUTS FROM THE RECEIVING CRYSTAL OF AN ACOUSTICAL DELAY LINE WHEN
C THE TRANSMITTING CRYSTAL IS EXCITED BY AN ARBITRARY DRIVING SIGNAL.
C ALTHOUGH THE PROGRAM WAS DESIGNED PRIMARILY FOR IMPULSE SIGNALS, IT
C WILL WORK EQUALLY WELL FOR CONTINUOUS SIGNALS.
C THE PROGRAM COMPUTES THE FIRST 13 PRESSURE WAVEFORMS, P10, THROUGH
C P113, AND THEREFORE THE FIRST 7 VOLTAGES, E10 THROUGH E13. THESE
C NUMBERS CAN EASILY BE INCREASED BY MODIFYING THE CARDS NUMBERED 50
C AND 60 AS WELL AS THE DIMENSION STATEMENTS.
C THE FOLLOWING PROCEDURES SHOULD BE FOLLOWED WHEN UTILIZING THIS
C PROGRAM.
C 1) CARDS 1 THROUGH 4 ARE TO BE USED TO BUILD AN ARRAY, V(N),
C OF VOLTAGES, EQUALLY SPACED IN TIME. THE UNIT OF TIME BEING
C ONE SIXTH THE TIME OF FLIGHT IN THE CRYSTAL. THEREFORE,
C EACH GROUP OF SIX VOLTAGES COMPLETELY FILL THE CRYSTAL.
C 2) THE THREE IMPEDANCES MUST BE SPECIFIED AS FOLLOWS.
C 5 Z1= IMPEDANCE OF THE FLUID IN THE WAVEGUIDE.
C 6 Z = IMPEDANCE OF THE CRYSTAL.
C 7 Z2= IMPEDANCE OF THE BACKING MEDIA.
C 3) THE FIRST AND LAST VOLTAGE TO BE PLOTTED MUST BE SPECIFIED
C USING CARDS 8 AND 9.
C 8 LOOK1= THE FIRST VOLTAGE PLOTTED.
C 9 LOOK2= THE LAST VOLTAGE PLOTTED.
C DIMENSION V(500),PP(500,13),EE(500,13)
C THE FOLLOWING 6 CARDS, PLUS ONE DATA CARD PUTS IN THE VOLTAGE FUNCTION
C 1 V(1)=1.00
C V(2)=0.00
C DO 3 N=3,500
C 3 V(N)=V(N-1)
C CONTINUE
C 4 CONTINUE
C NOTE V(N) DOES NOT INCLUDE THE CONSTANT A (SEE THEORY)
C 5 Z1=1.48231E+06
C 6 Z= 1.52000E+07
C 7 Z2= 4.15000E+02

```

FR 1=21

```

8 LOOK1=1
9 LOOK2=5
A1=Z1/Z
A2=Z2/Z

C A1 AND A2 IN PROGRAM REPRESENT M1 AND M2 IN THEORY
T1=(2.0*A1)/(A1+1.0)
T2=(2.0*A2)/(A2+1.0)
R1=(A1-1.0)/(A1+1.0)
R2=(A2-1.0)/(A2+1.0)
B1=A1/(1.0+A1)
B2=-1.0/(1.0+A2)
B3=-1.0/(A1-1.0)
R1R2=R1*R2

C COMPUTE THE INITIAL PRESSURE OUTPUT (P10) FROM THE FIRST CRYSTAL
M=5
INDEX=1
DO 11 N=INDEX,M
11 PP(N,1)=B1*V(N)
INDEX=INDEX+6
DO 12 N=INDEX,M
12 PP(N,1)=PP(N,1)+B2*T1*V(N+1-INDEX)
IFXP=0
13 IEXP=IEXP+1
INDEX=INDEX+6
DO 14 N=INDEX,M
14 PP(N,1)=PP(N,1)+B3*T1*V(N+1-INDEX)*(R1R2)**IEXP
INDEX=INDEX+6
DO 15 N=INDEX,M
15 PP(N,1)=PP(N,1)+B2*T1*V(N+1-INDEX)*(R1R2)**IEXP
IF(INDEX + 12 - 500) 13,21,21
21 CONTINUE
C1=-T1/A1

C NOTE C1 DOES NOT INCLUDE D11,R, OR C0 IN THE NUMERATOR OR Z IN THE
C DENOMINATOR (SEE THEORY)
C2=-C1*T2/A2
C3=-(C1*T1)/(A1*R1)

C STATEMENTS 50 THROUGH 59 WILL COMPUTE THE REMAINING PRESSURE PACKETS
LOCK=2*(LOOK2)-1

```

```

50 DO 59 NN=2,LOCK
INDEX=1
M=5
IFXP=0
DO 51 N=INDEX,M
51 PP(N,NN)=-R1*PP(N,NN-1)
52 INDEX=INDEX+12
DO 53 N=INDEX,M
53 PP(N,NN)=PP(N,NN)+T1**2*(R2/A1)*PP(N+1-INDEX,NN-1)*(R1R2)**IEXP
IFXP=IEXP+1
IF(INDEX+12-500) 52,59,59
59 CONTINUE
C STATEMENTS 60 THROUGH 69 WILL COMPUTE THE OUTPUT VOLTAGE PACKETS
60 DO 69 NN=1,LOCK,2
INDEX=1
M=5
DO 61 N=INDEX,M
61 EE(N,NN)=C1* PP(N,NN)
INDEX=INDEX + 6
DO 62 N=INDEX,M
62 EF(N,NN)=EE(N,NN) + C2*PP(N+1-INDEX,NN)
IFXP=0
66 IEXP=IEXP+1
INDEX=INDEX+6
DO 63 N=INDEX,M
63 EE(N,NN)=EE(N,NN)+C3*PP(N+1-INDEX,NN)*(R1R2)**IEXP
INDEX=INDEX+6
DO 64 N=INDEX,M
64 EF(N,NN)=EE(N,NN)+C2*PP(N+1-INDEX,NN)*(R1R2)**IEXP
IF (INDEX + 12 - 500) 66,69,69
69 CONTINUE
C STATEMENTS 73 THROUGH 76 WILL PRINT OUT THE VOLTAGES VALUES OF THE
C SEVEN VOLTAGE PACKETS COMPUTED.
73 PRINT 74
74 FORMAT(1H ///)
PRINT 75
750FORMAT(112H N E10(N) E12(N) E14(N)
1 E16(N) E18(N) E110(N) E112(N))

```



# APPENDIX II

Voltage Pulses within E , for Distilled Water at 21°C.

CALCULATED AMPLITUDES (Arbitrary Units)	CALCULATED VOLTAGES	MEASURED VOLTAGES
1 -0.1619 v.	-0.341 mv.	-0.311 mv.
2 +0.6477	+1.370	+1.283
3 -1.2377	-2.610	-2.472
4 +1.7127	+3.612	+3.470
5 -2.0879	-4.403	-4.186
6 +2.3786	+5.016	+4.799
7 -2.5967	-5.476	-5.179
8 +2.7537	+5.808	+5.556
9 -2.8586	-6.029	-5.706
10 +2.9203	+6.159	+5.864
11 -2.9454	-6.212	-5.854
12 +2.9406	+6.202	+5.932
13 -2.9110	-6.139	-5.795
14 +2.8615	+6.035	+5.749
15 -2.7958	-5.896	-5.562
16 +2.7175	+5.731	+5.484
17 -2.6295	-5.546	-5.255
18 +2.5344	+5.345	+5.103
19 -2.4340	-5.133	-4.871
20 +2.3304	+4.915	+4.731
21 -2.2250	-4.693	-4.455
22 +2.1189	+4.469	+4.292
23 -2.0133	-4.246	-4.034
24 +1.9090	+4.026	+3.899
25 -1.8066	-3.810	-3.640
26 +1.7067	+3.599	+3.509
27 -1.6098	-3.395	-3.257
28 +1.5161	+3.197	+3.112
29 -1.4258	-3.007	-2.868
30 +1.3392	+2.824	+2.729
31 -1.2564	-2.650	-2.525
32 +1.1774	+2.483	+2.405
33 -1.1022	-2.325	-2.198
34 +1.0308	+2.174	+2.118
35 -0.9631	-2.031	-1.937
36 +0.8991	+1.896	+1.876
37 -0.8386	-1.769	-1.685
38 +0.7816	+1.648	+1.640

## APPENDIX III

Voltage Pulses within E , for Distilled Water at 21°C.

CALCULATED AMPLITUDES (Arbitrary Units)		CALCULATED VOLTAGES	MEASURED VOLTAGES
1	-0.1095	-0.231 mv.	-0.148 mv.
2	+0.4379	+0.924	+0.655
3	-0.7507	-1.583	-1.198
4	+0.8131	+1.715	+1.390
5	-0.6987	-1.474	-1.198
6	+0.4806	+1.014	+0.842
7	-0.2013	-0.425	-0.350
8	-0.0967	-0.204	-0.143
9	+0.3910	+0.825	+0.646
10	-0.6594	-1.391	-1.081
11	+0.8921	+1.881	+1.483
12	-1.0796	-2.277	-1.803
13	+1.2198	+2.573	+2.029
14	-1.3107	-2.764	-2.177
15	+1.3544	+2.856	+2.383
16	-1.3533	-2.854	-2.227
17	+1.3116	+2.766	+2.185
18	-1.2336	-2.602	-2.046
19	+1.1242	+2.371	+1.874
20	-0.9984	-2.106	-1.620
21	+0.8310	+1.753	+1.372
22	-0.6569	-1.385	-1.046
23	+0.4704	+0.992	+0.772
24	-0.2757	-0.582	-0.443
25	+0.0763	+0.161	+0.124
26	+0.1242	+0.262	+0.181
27	-0.3232	-0.682	-0.498
28	+0.5178	+1.092	+0.848
29	-0.7063	-1.490	-1.136
30	+0.8865	+1.870	+1.469
31	-1.0573	-2.230	-1.731
32	+1.2174	+2.567	+2.044
33	-1.3660	-2.881	-2.300
34	+1.5025	+3.169	+2.546
35	-1.6265	-3.430	-2.766
36	+1.7379	+3.665	+2.964
37	-1.8366	-3.873	-3.146
38	+1.9227	+4.055	+3.290
39	-1.9967	-4.211	-3.385
40	+2.0587	+4.342	+3.503
41	-2.1093	-4.449	-3.562
42	+2.1490	+4.532	+3.640
43	-2.1783	-4.594	-3.666
44	+2.1979	+4.635	+3.692
45	-2.2084	-4.658	-3.722
46	+2.2104	+4.662	+3.740
47	-2.2040	-4.648	-3.710
48	+2.1917	+4.622	+3.657



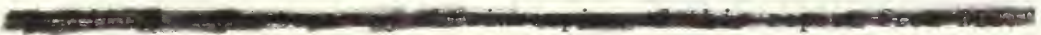
# INITIAL DISTRIBUTION LIST

	No. Copies
1. Defense Documentation Center Cameron Station Alexandria, Virginia 22314	20
2. Library U.S. Naval Postgraduate School Monterey, California 93940	2
3. Bureau of Naval Weapons Department of the Navy Washington, D.C. 20360	1
4. Prof. A. B. Coppens Department of Physics U.S. Naval Postgraduate School Monterey, California 93940	5
5. Lt. James E. Sheehan, USN P.O. Box 11 Elton, Penna.	3



## DOCUMENT CONTROL DATA - R&amp;D

(Security classification of title, body of abstract and indexing annotation must be entered when the overall report is classified)

1. ORIGINATING ACTIVITY (Corporate author) Ordnance Engineering Programs U.S. Naval Postgraduate School		2a. REPORT SECURITY CLASSIFICATION Unclassified	
		2b. GROUP	
3. REPORT TITLE Measurement of Acoustical Impedances of Fluids by Analysis of Transient Acoustic Waveshapes Using an Acoustical Waveguide with Piezoelectric Transducers.			
4. DESCRIPTIVE NOTES (Type of report and inclusive dates) Thesis			
5. AUTHOR(S) (Last name, first name, initial) SHEEHAN, James E.			
6. REPORT DATE	7a. TOTAL NO. OF PAGES 63	7b. NO. OF REFS 13	
8a. CONTRACT OR GRANT NO.		9a. ORIGINATOR'S REPORT NUMBER(S) 1	
b. PROJECT NO. N/A			
c.		9b. OTHER REPORT NO(S) (Any other numbers that may be assigned this report)	
d.			
10. AVAILABILITY/LIMITATION NOTICES 			
11. SUPPLEMENTARY NOTES		12. SPONSORING MILITARY ACTIVITY	
13. ABSTRACT A method has been developed for measuring the acoustic impedance of fluids in a fluid-filled waveguide terminated at each end by piezoelectric crystals. Output voltage waveforms were computed for the general case of an arbitrary driving voltage. Analysis of these output waveforms, when the driving voltage was an impulse function, indicated significant changes in the voltage envelopes as the acoustic impedance of the fluid within the waveguide was varied. The time of the first and second phase changes in the second received echo were plotted as a function of fluid impedance. Test fluids were analyzed with an impedance range of from $0.66 \times 10^6$ rayls to $19.7 \times 10^6$ rayls. The experimental results using the time of the second axis crossing or phase change as the test criterion, indicated that the acoustic impedance can be measured with the following accuracies:  a. 0.5 percent in the neighborhood of $Z = 0.66 \times 10^6$ rayls. b. 0.9 percent in the neighborhood of $Z = 1.50 \times 10^6$ rayls. c. 2.0 percent in the neighborhood of $Z = 2.50 \times 10^6$ rayls.			

14. KEY WORDS	LINK A		LINK B		LINK C	
	ROLE	WT	ROLE	WT	ROLE	WT
Impedance Acoustic Impedance Specific Acoustic Impedance Fluid Acoustic Impedance Acoustic Measurement						

### INSTRUCTIONS

**1. ORIGINATING ACTIVITY:** Enter the name and address of the contractor, subcontractor, grantee, Department of Defense activity or other organization (*corporate author*) issuing the report.

**2a. REPORT SECURITY CLASSIFICATION:** Enter the overall security classification of the report. Indicate whether "Restricted Data" is included. Marking is to be in accordance with appropriate security regulations.

**2b. GROUP:** Automatic downgrading is specified in DoD Directive 5200.10 and Armed Forces Industrial Manual. Enter the group number. Also, when applicable, show that optional markings have been used for Group 3 and Group 4 as authorized.

**3. REPORT TITLE:** Enter the complete report title in all capital letters. Titles in all cases should be unclassified. If a meaningful title cannot be selected without classification, show title classification in all capitals in parenthesis immediately following the title.

**4. DESCRIPTIVE NOTES:** If appropriate, enter the type of report, e.g., interim, progress, summary, annual, or final. Give the inclusive dates when a specific reporting period is covered.

**5. AUTHOR(S):** Enter the name(s) of author(s) as shown on or in the report. Enter last name, first name, middle initial. If military, show rank and branch of service. The name of the principal author is an absolute minimum requirement.

**6. REPORT DATE:** Enter the date of the report as day, month, year, or month, year. If more than one date appears on the report, use date of publication.

**7a. TOTAL NUMBER OF PAGES:** The total page count should follow normal pagination procedures, i.e., enter the number of pages containing information.

**7b. NUMBER OF REFERENCES:** Enter the total number of references cited in the report.

**8a. CONTRACT OR GRANT NUMBER:** If appropriate, enter the applicable number of the contract or grant under which the report was written.

**8b, 8c, & 8d. PROJECT NUMBER:** Enter the appropriate military department identification, such as project number, subproject number, system numbers, task number, etc.

**9a. ORIGINATOR'S REPORT NUMBER(S):** Enter the official report number by which the document will be identified and controlled by the originating activity. This number must be unique to this report.

**9b. OTHER REPORT NUMBER(S):** If the report has been assigned any other report numbers (*either by the originator or by the sponsor*), also enter this number(s).

**10. AVAILABILITY/LIMITATION NOTICES:** Enter any limitations on further dissemination of the report, other than those

imposed by security classification, using standard statements such as:

- (1) "Qualified requesters may obtain copies of this report from DDC."
- (2) "Foreign announcement and dissemination of this report by DDC is not authorized."
- (3) "U. S. Government agencies may obtain copies of this report directly from DDC. Other qualified DDC users shall request through \_\_\_\_\_."
- (4) "U. S. military agencies may obtain copies of this report directly from DDC. Other qualified users shall request through \_\_\_\_\_."
- (5) "All distribution of this report is controlled. Qualified DDC users shall request through \_\_\_\_\_."

If the report has been furnished to the Office of Technical Services, Department of Commerce, for sale to the public, indicate this fact and enter the price, if known.

**11. SUPPLEMENTARY NOTES:** Use for additional explanatory notes.

**12. SPONSORING MILITARY ACTIVITY:** Enter the name of the departmental project office or laboratory sponsoring (paying for) the research and development. Include address.

**13. ABSTRACT:** Enter an abstract giving a brief and factual summary of the document indicative of the report, even though it may also appear elsewhere in the body of the technical report. If additional space is required, a continuation sheet shall be attached.

It is highly desirable that the abstract of classified reports be unclassified. Each paragraph of the abstract shall end with an indication of the military security classification of the information in the paragraph, represented as (TS), (S), (C), or (U).

There is no limitation on the length of the abstract. However, the suggested length is from 150 to 225 words.

**14. KEY WORDS:** Key words are technically meaningful terms or short phrases that characterize a report and may be used as index entries for cataloging the report. Key words must be selected so that no security classification is required. Identifiers, such as equipment model designation, trade name, military project code name, geographic location, may be used as key words but will be followed by an indication of technical context. The assignment of links, roles, and weights is optional.









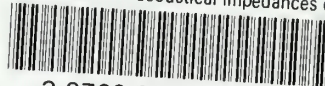






thesS4376

Measurement of acoustical impedances of



3 2768 001 94409 3

DUDLEY KNOX LIBRARY